Energy Policy 179 (2023) 113626

Contents lists available at ScienceDirect

Energy Policy

journal homepage: www.elsevier.com/locate/enpol

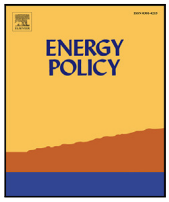

Research article

Energy, power, and greenhouse gas emissions for future transition scenarios

L. Battisti

DICAM, Department of Civil, Environment and Mechanical Engineering - University of Trento, via Mesiano 77, I-38050 Povo (TN), Trento, Italy

ARTICLE INFO

Keywords:
Energy transition
GHE
Renewable energy

ABSTRACT

Under the pressure for new policy and socio-ecological transformation, this work evaluates the future (2020–2050) GHG emissions, considering a likely range of electric energy growth scenarios in the world's current energy system. An integrated model accounts for different penetration strategies of renewable energies, technological advancements, and variations in the fuel/renewables mix. Data of actual renewable/fossil share, GHG emission factors, and technology indicators, as plant load factors, were assumed from the Italian scenario. The study reveals that regardless of the current electric energy demand for the future, the transition to a massive penetration share of renewables as unique GHG reduction strategy will only partially abate the level of GHGs, and the zero-emission targets are definitely not feasible. A relevant result is the evaluation of future green power capacity, to satisfy the worldwide electrical energy demand. The scenarios foresee an unprecedented rate of the installation of generation plants from renewable sources, accompanied by a steep year-by-year variation of the required power capacity in operation. This prediction, in the temporal front chosen for this survey, poses the problem of the technological readiness of many conversion technologies, which makes it difficult to guarantee that renewable penetration programs can be matched with their technical feasibility.

1. Introduction

1.1. Tackling the climate and environmental challenges

Since the beginning of the 21st century, the international scientific and geopolitical debate has centred on climate change caused by anthropogenic activity (IPCC, 2006). Global warming is having a devastating impact on ecosystems with unpredictable fallouts on economic development. Societal pressure and climate strikes by the young, have pushed governments to take action to strengthen the mitigation of greenhouse gas emissions, which are recognized as being majorly responsible for climate change, as claimed in the latest Special Report on Global Warming of 1.5 °C (SR1.5) (IPCC, 2018). Although carbon dioxide (CO_2) makes up the majority of the sector's greenhouse gas emissions, fractions of methane (CH_4), water, and nitrous oxide (N_2O) are also contributing to the global effect, in fact, CO_2 emissions account for approximately 76% of total greenhouse gas emissions (GHGs) (C2ES, 2021). Therefore the most relevant metric for air pollution, GHG emissions, instead of CO_2 emissions, is considered in this study as a more accurate indicator of air pollution for policymakers. Among various political actions, the European Green Deal (EGD) (EU, 2021) indicates as key points of its strategy low-carbon infrastructural development and digital transition, circular economy action plan, carbon pricing reform, energy efficient building renovation, rapid implementation of smart mobility solutions, ending fossil fuel subsidies, and innovating 'farm to fork' environmentally-friendly food systems. All these fields of intervention can be grouped into two broad classes, energy efficiency (building, transport, industrial/agricultural transformation) aimed to reduce the environmental impact of the end user's and the energy conversion processes.

1.2. The role of electricity consumption

Among the leading sources of GHGs is the electricity production sector, which handles the generation, transmission, and distribution of electricity, (IPCC, 2014), accounting for not less than 30% of the global share (IEA, 2019). The escalating growth of electricity consumption among end users will make the weight of this sector increasingly important in national energy systems. In Italy, since 2001 the energy consumption of the electricity sector has increased at higher rates than gross domestic consumption, which is an indication of the progressive electrification of final consumption services. The gross national production of electricity in Italy from 1990 to 2019 went from 216.6 TWh to 293.9 TWh with an increase of 35.7%. Electricity consumption went from 218.8 TWh to 301.8 TWh in the same period with an increase of 37.9%[1] (TERNA, 2020). The electricity is distributed to final users such

E-mail address: lorenzo.battisti@unitn.it.

[1] The difference in the balance being supplied by imports.

https://doi.org/10.1016/j.enpol.2023.113626
Received 9 July 2022; Received in revised form 13 April 2023; Accepted 11 May 2023
Available online 25 May 2023

Nomenclature

Acronyms

AEP	Annual Energy Production [kWh/year]
EGD	European Green Deal
GHG	GreenHouse Gas
LCA	Life Cycle Analysis
$PMGE$	Power Marginal Growth Factor [–]
PV	Photovoltaic
SFC	Specific Fuel Consumption [kg/kWh]

Greek letters

α	growth constant
α_d	de-growth constant
η	efficiency
γ	Pearl-Reed constant

Pedex

c	construction
d	decommissioning
f	fossil, fossil fuelled plants
$inst$	installed
j	LCA individual macro phase
N	number of fuel species
n	fuel specie
$O\&M$	operation and maintenance
r	renewable
ref	reference time period
t	time
T_0	year 0
T_{30}	year 30
$target$	target

Main symbols

a_f	energy attenuation factor
c	intensity factor during plant build-up phase
$CO_{2,eq}$	equivalent CO_2
d	intensity factor during plant decommissioning phase
E	electric energy [kWh]
e_1	variation of fossil to total electric energy use
e_2	share of the fuel energy contribution to the total
f	emission factor [kg_{CO_2}/MWh]
F_0	penetration level of renewable sources at $t = t_0$
f_{CO_2}	electric energy to CO_2 conversion factor [kg_{CO_2}/MWh]
g_{CO_2}	fuel to CO_2 conversion factor [kg_{CO_2}/kg_f]
i	growth rate [–]
i_0	reference growth rate [–]
K	constant
k_p	constant of period growth function
LF	plant load factor [–]
M	mass [kg]
o	intensity factor during plant operating phase
p	electric power [kW]
r	constant
T	year

as residential houses, commercial properties, businesses (e.g., heating, ventilation, air conditioning, lighting, and appliances), industries, and small factories, and finally transportation. As a consequence, it is legitimate to attribute the GHG from electricity generation to any sector whose energy demand makes use of electric energy. Since the electric vector is destined to continue into the future, tracking its evolution is indispensable for planning and monitoring initiatives aimed at reducing greenhouse gas emissions, and the development of containment strategies at national and local levels. As an extreme scenario, IEA forecasts a target of 90% of electric energy possibly generated by renewables by 2050 (IEA, 2021b). The evolution to a highly efficient electricity market copes well with renewable energies, and in a future of highly interconnected grids reaching instantaneous needs of final users, their intermittent nature will be less and less a deal. Already in 2020, 38% of the electricity consumption of the European Union was provided by renewable source plants (nd Energiewende and Ember, 2021), which thus surpassed fossils, while on a global level, it reached 29% (IEA, 2021a).

1.3. GHG emission scenarios

A quantitative analysis of future GHG has been attempted by several organizations, dating back to the 2000 IPCC by Nakicenovic et al. (2000). Such reports discuss how to keep the temperature rise below the threshold of 1.5 °C relative to pre-industrial levels, and indicate the pathways of mid to long-term behavioural societal transformation required to contain the carbon budget within this limit. Despite the different hypotheses and models used, leading to a very broad range of scenarios, two common points of consensus emerged: (i) the growth in electric energy demand is driven by the growth in per capita income as the main determinant of future emissions. This dynamic measure (unfortunately an ex-post assessment) is a consistent indicator of the growth in energy demand. At the same time, (ii) this parameter introduces a great source of uncertainty, as it is derived from the complex combination of multiple economic, technological, and demographic factors. Many papers deal with the problem of the future impacts of today's energy choices by analysing the problem based on political energy development plans, investment choices, and strategies for containing climate-altering emissions and sustainability objectives (American and Scientific, 2018; Tudor and Sova, 2021; UNFCCC, 2021b,a; DeutscheWelle, 2020; UNCCC, 2021; EEA, 2021; UN, 2021; UNCCC, 2019; IEA, 2021c; Wen and Yuan, 2020).

Following the guidelines of the largest supranational institutions, each country has adopted plans for an overall reduction in emissions of GHG to achieve the emission targets. This goal is pursued by several strategies: the improvement in energy conversion processes that determine a reduction in specific fuel consumption (energy efficiency measures in industry and buildings), the introduction of renewable sources in the energy system, the introduction of tailored energy policies (e.g., carbon tax, incentives for renewable sources), and finally the introduction of decarbonization technologies.

The fundamental contribution, in massive terms, given by renewable plants is represented by solar power (concentrated solar power, photovoltaic power), wind power sources through terrestrial and the offshore wind farms, potential geodetic power of water (head and runoff plants) with hydropower plants, and seawater (ocean currents, tidal) with hydrokinetic plants. A more marginal contribution is provided by geothermal power and wave/salt gradient power plants which are unfortunately very site-specific and characterized by low unit power if compared to previous plants. Although biomass fuel and biogas

electric power apparently have near-zero GHG emissions, they are characterized by a very low power per land surface unit, at least one order of magnitude lower than that of wind or solar power plants(Smil, 2015).

1.4. Current approaches to energy transition scenarios

Energy transition studies involve a large network of research areas, including the technology area (energy source exploitation, conversion, and supply, energy infrastructure planning), but also climate policy (environmental impact), and societal/economical transformation/organization policy (society organization and welfare, health, market behaviour, security of supply, etc.). A number of approaches and theoretical stands are used to conceptualize the phenomena, characteristics, and interaction levels of such areas (see for instance (del Granado et al., 2018; Halbe et al., 2015; Müllera et al., 2017; Li et al., 2015)). They differ according to level of complexity, and final scope (exploring transition path, providing policy advice, facilitating stakeholder decision processes, etc.). The review of these models is out of the scope of this study, and will not be discussed further. The literature body explored through major research engines and selected on the basis of similar area of investigation, considers primarily the measure of the GHG emissions, which is analysed according to three general approaches: the Primary Energy Equivalent (PEE) approach, the Equal Share (ES) approach, and the Index Decomposition Analysis approach. All models quantify the GHG emission savings GHG_s, according to the general model formalized in Eq. (1):

$$GHG_s = f_f \cdot \left(E - E_{T0}\right)_r \tag{1}$$

being f_f the emission factor [kg_{CO_2}/MWh] of fossil fuel plants, and $\left(E - E_{T0}\right)_r$ the non-fossil fuel electric energy generated in the period considered, where E_r is the energy target and $E_{T0,r}$ the baseline energy level. The avoided emissions assessed by Eq. (1) are then added to the emissions of the target year to obtain the total emission level (Clancy et al., 2015). PEE is a 'static' or 'stiff' approach as it generally considers the parameters of Eq. (1) as constant. In particular, the method does not account for the impact of operational changes to fossil fuel generators because of renewable generation. This method may over - or underestimate the fossil-fuel and GHG displacement as the impact of renewable energy tends to be focused on a subset of the generation portfolio, typically the more expensive or marginal power plants (Holttinen et al., 2014). It was adopted in 2015 by the European Environment Agency (Agency, 2015) as the method to consider any new renewable energy installation as a mean to avoid emissions that otherwise would have been emitted from fossil fuel plants. The emission factor of fossil generation is generally a weighted value and depends on the fossil generation mix and the emission factors of individual fossil fuels used in the given year in the country. ES (Goh and Ang, 2018) approach incorporates the ratio of the electricity demand in the target and base years, therefore is able to compute emission reductions based on changes in the share of non-fossil based electricity in the generation mix. Accordingly, Eq. (1) includes the rate of total energy demand E/E_{T0} as shown in Eq. (2):

$$GHG_s = f_f \cdot \left(\frac{E}{E_{T0}} E_r - E_{T0,r}\right) \tag{2}$$

Since the terms of Eq. (2) can be viewed as the single contribution of each non-fossil energy source, this approach allows also us to extend the measure by summing each of these contributions to obtain the total emission reduction arising from the substitution in the electricity mix of the share of non-fossil-based energy. Both PEE and ES approaches encounter two limitations. The first depends on the fact that emissions are weighted only based on the emission intensity of the target year, which consequently will weigh markedly on the forecast. They also do not take into account the baseline year's emission intensity, and therefore are not able to assess possible changes in emission intensities due to a change over time in the fuel mix, such as the transition from high fuel to carbon content to high to low carbon content (transition to natural gas or heavily hydrogenated fuels). A throughout comparison of these models with numerical examples is given in Goh and Ang (2018).

IDA approach (Ang, 2004; Xu and Ang, 2013) uses the classic economy decomposition methods to account (potentially) for all variables that determine 'dynamic' changes in GHG emissions during the period considered. The methods allow including several factors. Since the extension to 5-factor identity by considering, namely the activity, the structure, the energy intensity, the fuel mix, and the emission coefficient effects by Torvanger (1991) in 1991, the method has been widely used to carry out emission studies for many countries, especially for Far East economies. More than 900 emissions IDA studies have been reported in the peer review literature in the last ten years period (2013–2022) according to Mendeley statistics,[2] showing a growing escalation of related papers. Applications of the method for specific Countries can be found in Xu and Ang (2013, 2014), Zhang et al. (2013), Kim and Kim (2016), Yang et al. (2011). The model considers the contribution of the single n-fuel specie, forming the general Eq. (3):

$$GHG_s = \sum_{n=1}^{N} E \cdot \frac{E_f}{E} \cdot \frac{E_{f,n}}{E_f} \cdot \eta_f \cdot f_{f,n} = \sum_{n=1}^{N} E \cdot e_{1,n} \cdot e_{2,n} \cdot \eta_{f,n} \cdot f_{f,n} \tag{3}$$

or, by integrating the logarithms, the marginal variation of the saved GHG emissions can be expressed as a summation of the marginal increments/decrements (impacts) of the single contributions:

$$\frac{\Delta GHG_s}{GHG_s} = \frac{\Delta E}{E} + \sum_{n=1}^{N} \left(\frac{\Delta e_{1,n}}{e_{1,n}} + \frac{\Delta e_{2,n}}{e_{2,n}} + \frac{\Delta \eta_{f,n}}{\eta_{f,n}} + \frac{\Delta f_{f,n}}{f_{f,n}} \right) \tag{4}$$

$\frac{\Delta E}{E}$ is the marginal rate of electric energy use, $\frac{\Delta e_{1,n}}{e_{1,n}}$ is the marginal variation of fossil to total energy use, $\frac{\Delta e_{2,n}}{e_{2,n}}$ is the share of the n-fuel energy contribution to the total, $\frac{\Delta \eta_{f,n}}{\eta_{f,n}}$ is the marginal variation of fossil plant energy conversion efficiency, and $\frac{\Delta f_{f,n}}{f_{f,n}}$ is the marginal variation of the emission factor of the n-fuel.

A first limitation of the IDA model lies in the fact that plant efficiency, η_f is not a sufficiently informing parameter to assess technology advancements Another important limitation of this version of the IDA approach arises from the fact that it does not consider the, albeit low, GHG emission contribution of renewable energy conversion processes. In general also the emission factor, either fossil or renewable, should be based on the LCA of processes to have a more exhaustive view of the global environmental impact of the energy conversion technologies.

1.5. Paper outline

The study forecasts the contribution of electric energy generation to GHG emissions for a midterm scenario of 30 years in accordance with the standard governance projections to the year 2050. Although the electric energy demand scenarios are a consequence of various factors that contribute to economic growth (demographic, technological, behavioural, etc.), the author defines general trends, indicating a likely range of possible growth scenarios, without investigating the mechanisms that form the basis of the global construction of the demand itself. Of course, the generality of the model allows selecting any wished energy change scenario. It is also assumed that the energy demand is satisfied by transition roadmaps to renewable, where the plant's load factor is the indicator of the technology evolution. This parameter incorporates fuel availability, technology advancement, regulatory evolution, market strategies, and efficiency, being therefore a far more complete parameter to evaluate energy conversion technology readiness over time. As a consequence, the power plant capacity

[2] Mendeley, https://www.mendeley.com/; search for: Index Decomposition Analysis and emission, accessed January 2023.

required is inferred and the GHG emissions related to the production can be rigorously determined. The actual share of fossil-to-renewable energies, fuel mix, and fossil and renewable plants load factor are taken from the Italian scenario data.

The model uses four key indices for the discussion: (i) the demand for electricity from fossil and renewable sources for any transition scenarios; (ii) the demand for power plants to provide the energy demand; (iii) the marginal trend of power (essential for the decision to build/decommission plants in the future), and (iv) the consequent greenhouse effect in terms of GHG (expressed as $CO_{2,eq}$) emitted, and saved.

The model presented is an analytical model marching in time, built by nesting of submodels made by independent variables. The general path is given in Fig. 7 of Chapter 5. Section 2 introduces several electrical energy growth scenarios characterized by different growth rates. Fig. 4 shows these scenarios. In Section 3, two models of energy transition through which fossil sources are progressively replaced by renewable ones are used: (i) the 'forced' one (top-down approach, Fig. 5), where the decision-maker imposes the implementation of a roadmap of progressive (linearly increasing) penetration over thirty years. According to this strategy, the penetration of renewable sources in the electricity sector is a consequence of the policies to contain greenhouse gas emissions and the objectives of increasing the share of renewable energy in final consumption under given constraints. The roadmap can be implemented through measures such as incentives and priorities for dispatching electricity from renewable sources. Another approach is (ii) the 'liberal' energy transition (bottom-up approach, Fig. 6), where the penetration follows a typical logistic trend. Here a natural saturation level of penetration can be set with the achievement of 90% of total energy production by renewable sources in the time frame considered. This situation is driven by either endogenous and exogenous factors (social acceptance, market dynamics, environmental limits, technology advancements, etc.). This demand is corrected by intensity attenuation laws or other wished correction mechanisms (rebound effect, other economic mechanism) (Marchetti, 1977). The power capacity needed to fulfil the energy requirement is a consequence of the transition model adopted. As the energy and power evolution are computed, Section 4 introduces a model of greenhouse gas emissions that takes into account the specific characteristics of the plants (fossil or renewable), and advances in future technologies. As the GHG emission is partly due to electric energy production and part to power plant commissioning/decommissioning, and operation, both energy and power output are used to compute GHG emission, by means of suitable emission factors inferred from LCA analysis (see Tables 3, 4 and 5). Section 5 presents the basic assumptions and the limitations of the model and discusses the results of the adoption of different growth scenarios on the electricity demand (energy and power) and environmental effects (greenhouse gas emissions). The most interesting combinations of these models generated 17 scenarios commented on in the Discussion. Section 6 presents a sensitivity analysis to evaluate the weight of the assumption drawn from the model's general results. Section 7 presents the conclusions. The model can handle either positive and negative variation of all the quantities over time, to correctly compute each contribution, and since its general, and flexible structure is easily implementable in a worksheet to allow extensive parametric analysis to be carried out.

2. Growth model of energy and power

If the electric energy needs are satisfied by the electric energy production E, under the hypothesis that the demand grows over time at the same constant annual rate, i, the variation is:

$$\frac{dE}{dt} = E \cdot i \tag{5}$$

and by integration, an exponential growth model can be obtained, governed by the annual growth rate i, with a linearly increasing attenuation factor law f(a_f):

$$E_t = E_{T_0} e^{i(t-T_0)} \left[1 - f(a_f)\right] \tag{6}$$

where E_t is the electricity produced at year, t and E_{T_0} is the electrical energy produced at the initial year T_0. The power to be installed to supply the electricity produced amounting to E_t can be calculated on the basis of the plant load factor LF:

$$P_{inst} = \frac{E_t}{LF(t) \cdot T} \tag{7}$$

where T refers typically to one year or 8760 h.

As the energy and power are calculated, the power marginal growth factor ($PMGF$) can be derived:

$$PMGF = \frac{P_{t+1} - P_t}{P_t} \tag{8}$$

To generate likely electrical energy growth scenarios, the historical data provided by BP (2020) were analysed to obtain an indication of the trend in electric energy generation from 1990 to 2020 for the main countries in the world. Eq. (5) was used to compute the growth rate i. The results in Fig. 1 show the emerging scenarios of continents, and relevant sub-regions. Some present an almost constant electric energy growth rate, with different intensities, ranging from 1% (i.e. Europe) to about 9% (China), or even slightly decreasing. Some countries such as CIS (Azerbaijan, Belarus, Kazakhstan, Russian Federation, Turkmenistan, USSR, Uzbekistan) and other European members (Albania, Bosnia-Herzegovina, Bulgaria, Croatia, Cyprus, the former Yugoslav Republic of Macedonia, Georgia, Gibraltar, Latvia, Lithuania, Malta, Montenegro, North Macedonia, Romania, and Serbia) show an escalating growth rate. Notable countertrends within the same geophysical/political regions can be occasionally noted, as shown in Figs. 2 and 3, which show more specifically the situations of South America and Europe. These data indicate other more complex trends, depending on the specific local political or environmental (availability of resources) situation, which analysis is beyond the scope of the paper. Nevertheless, these energy demand evolutions, which depend on endogenous and exogenous markets, and sociological and political factors, can be used to generate a range of realistic 'shapes' of future growth.

As consequence, the following generalized growth models can be used to cover all current and future global situations:

- models with a constant growth rate over time (i = const.). We arbitrarily defined: a low/normal growth rate can be defined as $i = 1 \div 2\%$ (or lower figures), a medium growth rate, $i = 3 \div 4\%$, and a high growth rate, $i = 7 \div 8\%$ (or higher figures). These models depict future scenarios with a very stable economic development, characterized by geopolitical stability and a definite supply of fossil and renewable sources.

$$i = const. \tag{9}$$

- models with increasing but attenuated exponential growth: this scenario is typical for countries experiencing an initial boom in economic growth, followed by a gradual settlement, i.e. countries with dynamic commercial interactions, and conspicuous energy resources ($\alpha < 1$, $i_0 = i_{T0}$, $i_{30} = i_{T30}$):

$$i = i_{30} - i_0 \cdot e^{(\alpha t)} \tag{10}$$

- models with periodic fluctuations characterized by constant average growth rates over the period considered, indicating cycles of increasing and decreasing demand, for example with a ten-year or twenty-year frequency (T_{ref}) oscillating around an average value i_0. These models are designed to describe a future situation when periodic pandemics, wars, or downturns in fuel supply will temporarily slow down the demand for electrical energy. For this scenario, 40 years was used as a time frame:

$$i = i_0 \left\{1 + sin\left(\pi/2 \cdot t/T_{ref}\right)\right\}$$

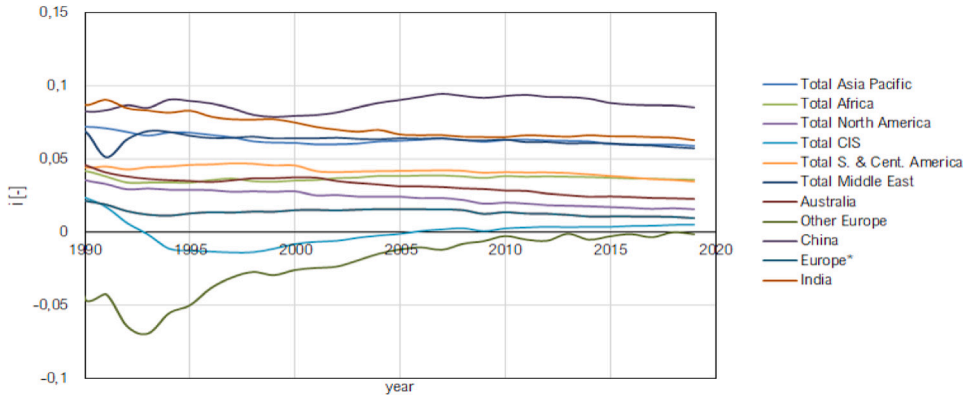

Fig. 1. Electric energy generation growth rate of the world's main countries in the period 1985–2020. Europe*: OECD members (Organization For Economic Co-operation and Development). Other European countries: Albania, Bosnia-Herzegovina, Bulgaria, Croatia, Cyprus, the former Yugoslav Republic of Macedonia, Georgia, Gibraltar, Latvia, Lithuania, Malta, Montenegro, North Macedonia, Romania, and Serbia. CIS: Azerbaijan, Belarus, Kazakhstan, Russian Federation, Turkmenistan, USSR, Uzbekistan. Elaboration of data BP (BP, 2020).

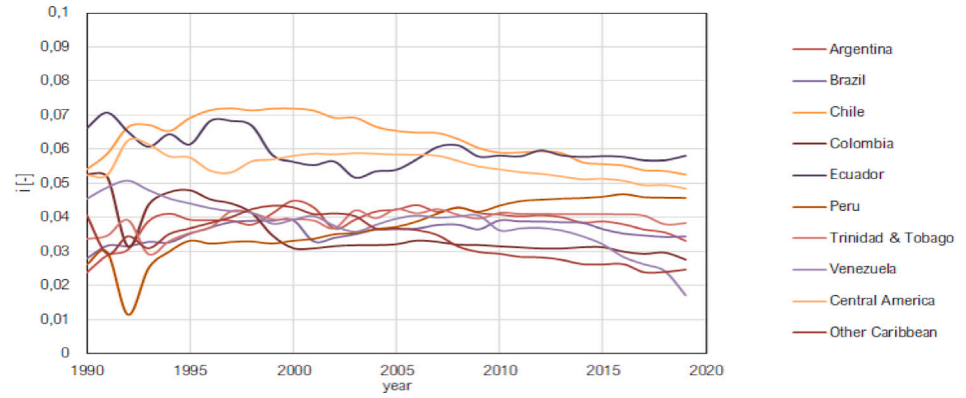

Fig. 2. Electric energy generation growth rate of South American countries in the period 1990–2020. Analysis of BP data (BP, 2020).

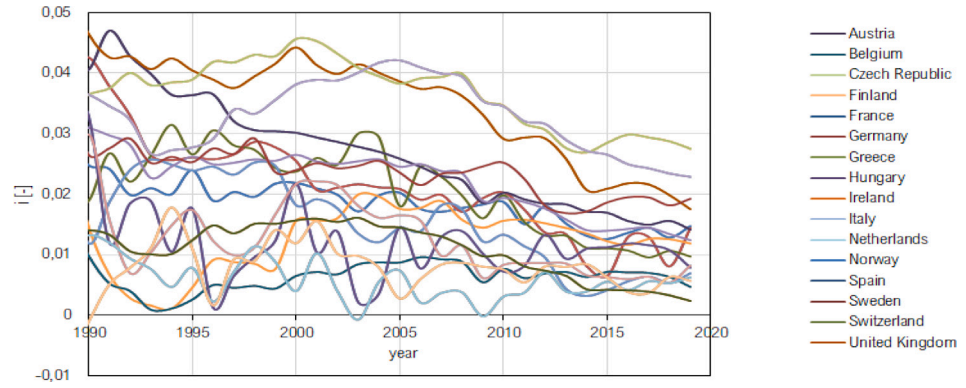

Fig. 3. Electric energy generation growth rate of European countries for 1990–2020. Analysis of BP data (BP, 2020).

- models with periodic growth rates, but characterized by fluctuations with average values dropping over time. These models are designed to model economic fluctuations with declining growth trends. Again, 40 years was used as a time frame:

$$i = i_0 \left\{ k_p \cdot t + sin\left(\pi/2 \cdot t/T_{ref}\right) \right\}$$

- according to the vision of degrowth (*decroissance*) of a planned downscaling of energy and resource use, additional scenarios were added to consider political resolutions aimed to contain the future energy demand. This vision tries to cope with the limits associated with the availability of natural resources (Meadows et al., 1972), and is discussed by a vivid ecology and social literature (Latouche, 2010) after the 1970s The model forces consumption in the long period to slow down to a target level by a linear drop in the growth rate ($\alpha_d > 1$).

$$i = i_0 \cdot e^{(-\alpha_d \cdot i_0 \cdot t)}$$

Fig. 4 shows the examples of these basic cases.

3. Energy transition models

3.1. Linear, constant energy transition model

Different laws of penetration of renewable sources through the progressive substitution of fossil fuels into the energy system can be

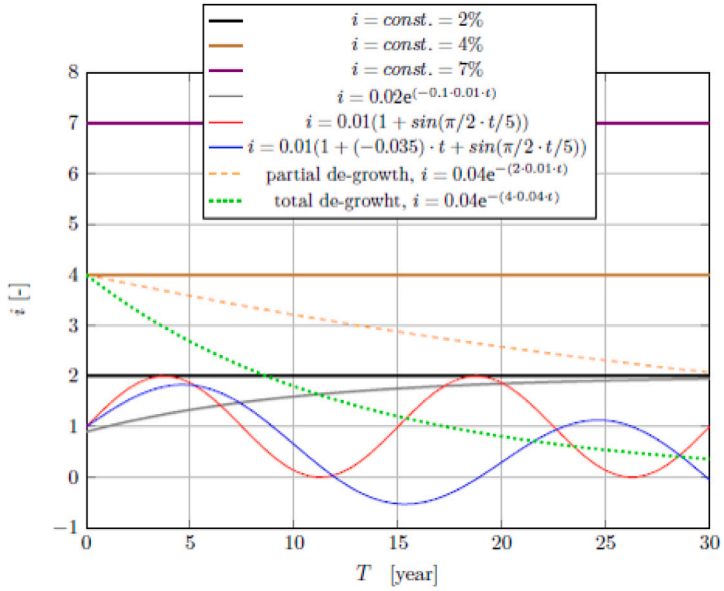

Fig. 4. Basic growth/de-growth models used for the simulations.

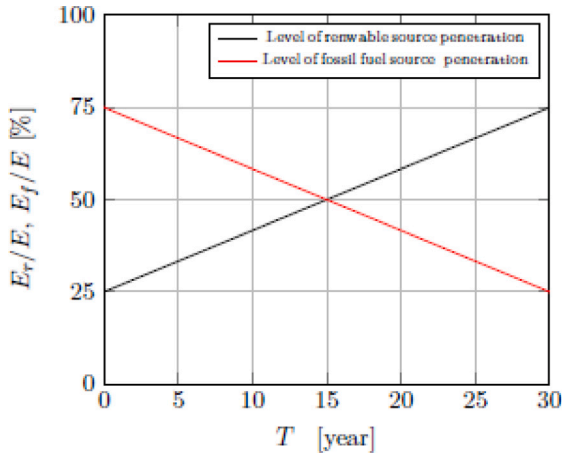

Fig. 5. Substitution model of fossil sources with the hypothesis of linear growth from the initial value of renewable contribution from 25% at year T_0 to 75% at the year T_{30}.

planned through mid to long-term strategies. For example, a possible top-down pathway can impose a constant rate of penetration of renewable sources into the energy system that varies from the initial value E_{T0} at the year T_0 to a target value $E_{target,r}$ to be achieved at year T_{30}. During this period, the fossil energies E_f will be substituted, generating a complementary trend. Therefore, at any instant, the electricity demand is satisfied by the production $E(t) = E_f + E_r$. Based on these assumptions, a linear model of penetration of the renewable sources is:

$$E_r = E_{T0,r} + \frac{E_{target,r} - E_{T0,r}}{\Delta t} \tag{11}$$

and:

$$E_f = E - E_r \tag{12}$$

corresponding to the one shown in Fig. 5, where $E_{T0,r} = 25\%$, and $E_{target,r} = 75\%$.

Linear substitution models suffer from at least two limiting factors in the transition process, as emerges from the analysis of economies historically based on the use of fossil fuels:

- *the operation of the electricity grid*; the connection of renewable source generation plants to the grid, with intermittent (even if partly predictable) and time-varying power levels, is equivalent, from an electrical point of view, to the insertion of sources of perturbation of the power level. This forces the grid control system to continuously compensate for fluctuations to avoid local disconnections of the electricity grid or, in the worst case, blackouts. The ability to manage perturbations depends on the mix of the technology used to generate the electrical load and the magnitude of the instantaneous loads. The interposition of energy storage systems increases the flexibility of use, and hence the penetration rate of renewable sources. The top-down approach must necessarily include scheduling technical updates. Although many papers have been published regarding penetration limits of renewables into the grid (Impram et al., 2020; Cochran et al., 2014; Burke and O'Malley, 2011), there is currently no conclusive data on the maximum penetration rate of intermittent sources, and the scenarios differ from country to country.

3.2. Logistic energy transition model

A model that is physically closer to a realistic renewable penetration trend is the logistic growth model, which belongs to the bottom-up type category. The penetration of renewable sources in the energy system is influenced by saturating factors, such as the natural limit of the availability of the renewable resource, the limits of the market and/or the regulatory context, and by the technology factors mentioned in the previous subsection. These factors determine the achievement of a characteristic, asymptotic, 'physiological' growth trend. Here a model of penetration of renewable source plants was used expressed by logistic functions, i.e. the one shown in Fig. 6, which refers to the well-known Pearl-Reed model (Pearl and Reed, 1920)

$$E_r(t) = \frac{E_{target,r} \dfrac{E_{T0,r}}{E_{T0}} e^{\gamma t}}{E_{target,r} + \dfrac{E_{T0,r}}{E_{T0}} (e^{\gamma t} - 1)} \tag{13}$$

where $E_{target} = 0.9$, and $\gamma = 0.2$. The model was therefore assumed to satisfy at T_{30} 90% of the total energy demand with renewables, starting

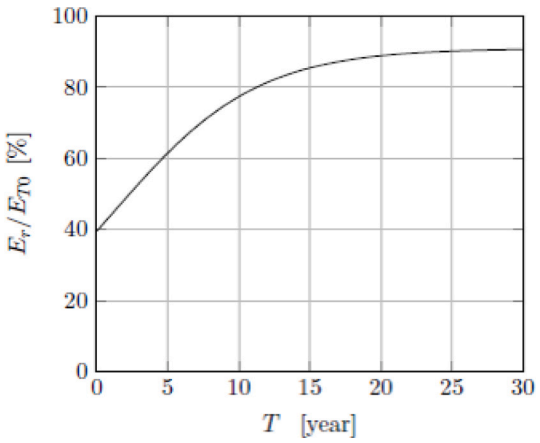

Fig. 6. Renewable penetration law according to the Pearl–Reed logistic model ($E_{target,r}$ = 90%, γ = 0.2, $E_{T0,r}/E_{T0}$ = 0.395).

from an arbitrary initial penetration level of $E_{T0,r}/E_{T0}$ = 39.5%[3] assumed at year T_0.

4. Greenhouse gas emission model

Each electric energy demand scenario has an impact in terms of equivalent carbon dioxide $CO_{2,eq}$ or greenhouse gas emission GHG deriving from the process of electric energy production. Conversion factors f (greenhouse gas warming potential GWP) are expressed in terms of kg of $CO_{2,eq}$ per MWh of electricity generated, both for fossil-fuelled plants and renewable fuelled plants. These factors account for emissions generated from all macro phases of the plant life cycle (Life Cycle Analysis approach - LCA), starting from the materials used for construction, through all of the lifespan operations, and finally of its disposal. This approach means that the mass of equivalent carbon dioxide produced during each j-phase can be quantified:

$$\left(M_{CO_2,eq}\right)_j = (f \cdot E)_j \tag{14}$$

where j is the individual macro-phase, and E the energy use associated with the specific activity. Despite some unsolved issues (Reap et al., 2008), the main methodology to compute the emission factor is the procedure regulated by the ISO 14040 Standard (principles and framework) (ISO, 2006), and the following issues.[4] According to the LCA approach, the entire GHG emissions account for the green warming potential factor generated by combustion f_f (which is zero for renewable source plants), and is often referred to as *direct emissions* or *stack emissions*, as well as *indirect emissions* that derive from the energy consumed due to construction (E_c), operation and maintenance ($E_{O\&M}$) and decommissioning/disposal (E_d) of the plant:

$$M_{CO_2,eq} = \sum_{j=1}^{J} \left(f \cdot E_f\right)_j = f_f \cdot E + f_c \cdot E_c + f_{O\&M} \cdot E_{O\&M} + f_d \cdot E_d \tag{15}$$

Emission factors from combustion f_f were provided in the 2006 IPCC Guidelines for National Greenhouse Gas Inventories (IPCC, 2006),[5] and updated in the 2019 Refinement version (IPCC, 2021). The factors refer to the stationary combustion in boilers and heaters. In addition, many papers provide independent evaluations (Hondo, 2005; Bouman, 2020; White and Kulcinski, 2000; Gagnona et al., 2002; Varun and Bhat, 2009; Dudhani et al., 2006; El-Fadel et al., 2003). These papers highlight that the emission factors change in line with evolutions in technologies (efficiency increase, material selection), and with the size and location of plants (altitude or latitude and by site-specific climatic variables such as temperature). GHG emissions vary also according to the country of production, primarily due to the differences in the fuel mix of the specific country. Table 1 indicates the change in the fuel mix occurring from 2005 to 2019 in Italy (ISPRA, 2021b).

As a result of improvements in energy conversion and the transition to natural gas, greenhouse gas emissions have gradually decreased over the years, as shown in Table 2. The emission factor for gross national thermoelectric production decreased steadily from 1990 to 2019, from 709 kg CO_2/MWh to 462 kgCO_2/MWh (ISPRA, 2021a) due to the increase in the fuel mix of the natural gas share. This was accompanied by an increase in the electrical conversion efficiency of plants fuelled by natural gas.

Several studies have measured the GHG emissions from renewable plants and compared them with fossil-fuelled plants. Specific conversion plants such as wind plants (Lenzen and Munksgaard, 2002; Bonou et al., 2016; Wang and Sun, 2012; Kabir et al., 2012), geothermal (Hammons, 2004), and sun (de Lima et al., 2021; Nishimura et al., 2010; Peng et al., 2013; Becker and Meinecke, 1992) provide evaluations of the emission factors. As no stack emissions are released, the contribution from plant construction, operation and decommissioning, is considerably smaller compared to fossil-fuelled plants. The electrical energy production of renewable plants (to a lesser extent for solar ones) is highly site-dependent, and the intermittency of the resource impacts on the load factor both spatially and temporally. The very fast evolution in technologies for renewable energy has led to a widespread range of emission factors observable in literature. Finally, also climate change gives rise to mid to long-term variations, because of its impact on natural resource availability. The collection of these data resulted in a range of values for each technology shown in Table 3. To compute a realistic measure of the GHG emitted by future renewable plants, the minimum values from cited studies are taken as a target, to account for the expected improvement in pollution mitigation of the processes.

As the different growth/degrowth scenarios depicted in Fig. 4 foresee phases when the electrical energy demand increases or decreases, the associated GHG emissions of both fossil and renewable plants are measured by the following models in Section 4.1. These models do not account for additional infrastructures (i.e. electric lines and substations, storage plants, etc.) necessary for additional electric energy dispatching and related energy losses.

4.1. GHG emissions for fossil fuel plants

CASE A

If the evolution of the demand is such that:

$$\begin{cases} \dfrac{dP_f}{dt} > 0, \\ P > P_{T_0} \end{cases}$$

the emissions are due to the operation and decommissioning of the installed fossil fuel plant capacity P_{T_0}, in operation at time T_0, plus the energy demand $(E - E_{T_0})_f$ required by the specific scenario, which gives rise to emissions for the construction, operation, and the end-of-life decommissioning of new plants. In terms of the amount of greenhouse gases produced, we therefore obtain:

$$GHG = \left(M_{CO_2,eq}\right)_{actual\ capacity} + \left(M_{CO_2,eq}\right)_{future\ capacity} \tag{16}$$

and in more detail:

$$GHG = f_f \cdot \left(P_{T_0} \cdot LF_{f,T_0} \cdot 8760\right) + \left[f_{CO_{2,eq}} \cdot E_{T_0}\right]_{O\&M} + \left[f_{CO_{2,eq}} \cdot E_{T_0}\right]_d \tag{17}$$

[3] data for Italy 2019 (Arera, 2019).

[4] ISO 14041 (1998) on goal and scope definition and inventory analysis, ISO 14042 (2000) on life cycle impact assessment, and ISO 14043 (2000) on life cycle interpretation.

[5] emissions arising from fuel combustion for energy production are reported under IPCC Table 1 A.

Table 1
Mix of fuel used for the thermoelectric production in Italy (2005–2019). (ISPRA, 2021b).

Year	2005	2010	2011	2012	2013	2014	2015	2016	2017	2018	2019
Type of fuel											
Solid	0.19	0.19	0.21	0.24	0.25	0.25	0.24	0.20	0.17	0.16	0.11
Natural gas	0.53	0.59	0.56	0.53	0.49	0.47	0.51	0.56	0.60	0.60	0.65
Gas derived	0.02	0.02	0.02	0.03	0.02	0.02	0.01	0.02	0.01	0.02	0.02
Oil products	0.21	0.13	0.11	0.10	0.09	0.09	0.08	0.07	0.07	0.07	0.06
Other fuels	0.04	0.07	0.10	0.11	0.15	0.17	0.15	0.15	0.15	0.16	0.16
Of which of fossil origin	0.97	0.94	0.92	0.91	0.87	0.85	0.87	0.87	0.87	0.87	0.86

Table 2
Emission factors of CO_2 from gross thermoelectric production by fuel ($kgCO_{2,eq}$/MWh).

Year	1990	1995	2000	2005	2010	2015	2016	2017	2018	2019
Total thermoelectric[a]	709,3	682.9	640.6	585.2	546.9	544.4	518.3	492.7	495.0	462.2

[a]Excluding electricity produced from biodegradable waste, biogas and vegetable biomass of plant origin (ISPRA, 2021a).

Table 3
GHG per electric MWh generated from main renewable source fuelled plants.

Renewable source	Type of plant	Min GHG emission [$kgCO_{2,eq}$/MWh]	Max GHG emission [$kgCO_{2,eq}$/MWh]
Water	Head Hydropower	10	300
Water	Runoff Hydropower	2	250
Wind	Offshore Wind farm	25	25
Wind	Inshore Wind farm	5	20
Sun radiation	PV farm	50	200
Sun radiation	CSP	30	75
Endogenous heat	Geothermal	25	300

$$+ f_f(t)\left[\left(P - P_{T_0}\right)\cdot LF(t)\cdot 8760\right] + \left[f_{CO_{2,eq}}\cdot\left(E - E_{T_0}\right)\right]_c + \left[f_{CO_{2,eq}}\cdot\left(E - E_{T_0}\right)\right]_{O\&M} + \left[f_{CO_{2,eq}}\cdot\left(E - E_{T_0}\right)\right]_d \quad [kgCO_{2,eq}]$$

Introducing the intensity factors of the construction, operation, and decommissioning phases of fossil plants:

$$c_f = \left(\frac{E_c}{E}(f_{CO_{2,eq}})_c\right) \quad [kgCO_{2,eq}/kWh]$$

$$o_f = \left(\frac{E_{O\&M}}{E}(f_{CO_{2,eq}})_{O\&M}\right) \quad [kgCO_{2,eq}/kWh]$$

$$d_f = \left(\frac{E_d}{E}(f_{CO_{2,eq}})_d\right) \quad [kgCO_{2,eq}/kWh]$$

one obtains:

$$GHG = f_f\cdot E_{f,T_0} + E\cdot\left[o_f + d_f\right] + f_f(t)\cdot\left(E - E_{T_0}\right) + \left[\left(E - E_{T_0}\right)\cdot\left(c_f + o_f + d_f\right)\right] \quad [kgCO_{2,eq}] \tag{18}$$

CASE B

If the evolution of the demand is such that:

$$\begin{cases}\frac{dP_f}{dt} < 0\\ P < P_{t_0}\end{cases}$$

the emissions are due to the operation of the fraction of the already installed capacity which uses the power $P < P_{t_0}$.

$$GHG = f_f\cdot E_{f,T_0} + E\cdot\left[o_f + d_f\right] \tag{19}$$

4.2. GHG emission for renewable plants

Analogously for emissions due to renewable plants, the following conditions can occur:

CASE C

$$\begin{cases}\frac{dP_r}{dt} > 0,\\ P > P_{T_0}\end{cases}$$

The emissions are due to the contribution of the operation and future decommissioning of the power P_{T_0} installed and in operation at time T_0 plus the additional emissions caused by the future requirement of new renewable power capacity $P - P_{T_0}$ which determines the emissions for its construction, operation, and disposal.

$$GHG = \left[f_{CO_{2,eq}}\cdot E_{T_0}\right]_{O\&M} + \left[f_{CO_{2,eq}}\cdot E_{T_0}\right]_d + \left[f_{CO_{2,eq}}\cdot\left(E - E_{T_0}\right)\right]_c + \left[f_{CO_{2,eq}}\cdot\left(E - E_{T_0}\right)\right]_{O\&M} + \left[f_{CO_{2,eq}}\cdot\left(E - E_{T_0}\right)\right]_d \quad [kgCO_{2,eq}] \tag{20}$$

Introducing the intensity factors of the construction, operation and decommissioning phases of renewable source plants:

$$c_r = \left(\frac{E_c}{E}(f_{CO_{2,eq}})_c\right) \quad [kgCO_{2,eq}/kWh]$$

$$o_r = \left(\frac{E_{O\&M}}{E}(f_{CO_{2,eq}})_{O\&M}\right) \quad [kgCO_{2,eq}/kWh]$$

$$d_r = \left(\frac{E_d}{E}(f_{CO_{2,eq}})_d\right) \quad [kgCO_{2,eq}/kWh]$$

one gets:

$$GHG = E_{T_0}\cdot\left[o_r + d_r\right] + \left(E - E_{T_0}\right)\cdot\left[c_r + o_r + d_r\right] \quad [kgCO_{2,eq}] \tag{21}$$

CASE D

If the evolution of the demand is such that:

$$\begin{cases}\frac{dE_r}{dt} < 0\\ P < P_{t_0}\end{cases}$$

the emissions are due to the operation of the already installed capacity which uses the power $P < P_{T_0}$ and it results:

$$GHG = E_{T_0}\cdot\left[o_r + d_r\right] \quad [kgCO_{2,eq}] \tag{22}$$

The intensity factors used for the simulations are shown in Table 4.

The emissions saved can be computed by:

$$GHG_s = \left(E - E_{T0}\right)_r\cdot\left[f_f + c_f + o_f + d_f\right] \quad [kgCO_{2,eq}]$$

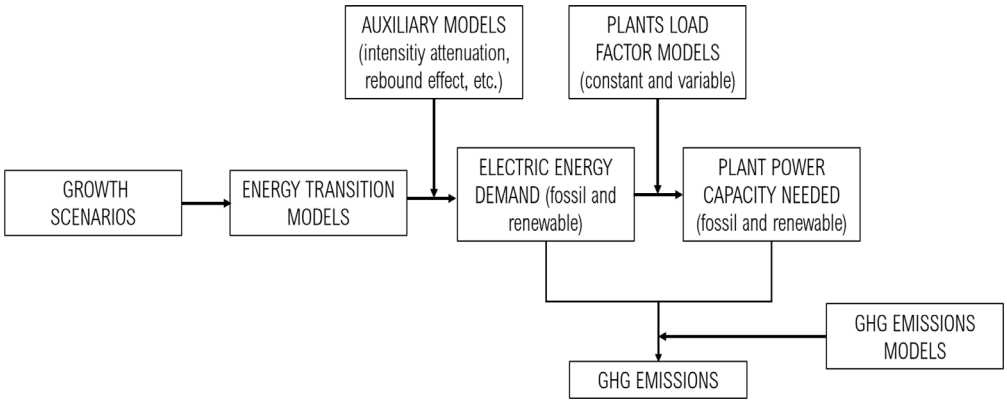

Fig. 7. Flow chart of the general model.

Table 4
Intensity factors of plant macro phases.

Type of plant	Fossil	Renewable
Fuel	$f_f = 0.80 \div 0.94$	$f_r = 0$
Construction	$c_f = 0.3 \div 0.5$	$c_r = 0.7 \div 0.8$
Operation	$o_f = 3.3 \div 19.5$	$o_r = 0.02 \div 0.2$
Decommissioning	$d_f = 0.3 \div 0.5$	$d_r = 0.1 \div 0.2$

5. Results and discussion

Some scenarios can be created by combining the models discussed above, covering almost all future changes in the demand for electrical energy, as shown in Fig. 1. The general model is organized according to the flowchart presented in Fig. 7, and the selected combinations for the discussion are listed in Table 6.

5.1. Assumptions underlying the general model

The basic assumptions underlying these models are:

- the time frame considered is 30 years (2020–2050)[6];
- the nuclear (both fusion and fission) sources are not used in the replacement scenarios;
- the CO_2 sequestration technologies are not considered
- to consider the two scenarios of constant and variable LF in the future. The load factor is defined as:

$$LF = \frac{E}{P_{inst} \cdot T} = \frac{\int^T P(t)dt}{P_{inst} \cdot T} \tag{23}$$

Constant LF could be typical of countries where a delay in the introduction of new conversion technologies is considered, or where there is a scarce availability of the source. For instance, countries with limited hydropower and wind resource can rely only or almost entirely on PV plants, therefore they will tend to assume the load factor of PV in the mid-long term period.
The future increase in the load factor of renewable and fossil-fuelled plants accounts for technological improvements (an increase of conversion efficiency, improvement of construction and maintenance technology, balancing of electrical loads through the introduction of storage systems), better localization of future plants (i.e. considering offshore technologies for wind farms) and a policy of priority dispatching of renewable energy. With regard to fossil-fuelled plants, implementing combined plants can significantly improve the load factor through the increase in the AEP. An increase in the load factor of fossils from the current 33% (EIA, 2022) to 45% (+36%) was considered in the simulations, while that of renewable source plants from 20% (BP, 2020) to 25% (+25%). For the sake of simplicity, this increasing trend is assumed to be linear over the period considered;

- it is assumed that at year T_0 1 MWh of electricity is produced, with 60.5% obtained from plants fuelled by fossil sources and 39.5% by renewable sources (the Italian scenario in 2019 has been taken as reference (Arera, 2019));
- it is hypothesized to introduce an attenuation factor of the increasing energy intensity over time, implemented through the improvement in the efficiency of the final use systems, the reduction of thermal losses, etc. According to the IEA (2020) report, since 2015, improvements in energy efficiency measured by primary energy intensity, have declined. The COVID-19 pandemic added a further level of criticality to the process. The energy intensity is expected to improve only by 0.8% in 2020, about half the rate, corrected for weather effects, of 2019 (1.6%) and 2018 (1.5%). It is therefore assumed that in the following 30 years, the demand for electricity for the processes decreases linearly up to a maximum value of 2.5% due to energy efficiency interventions. Rebound effects, which would partially offset the effect of the aforementioned energy efficiency trend, are neglected here, but could easily be implemented in the model. Evidence shows that general goods consumption in advanced economies resulting from lower energy costs will be modest in the context of global CO_2 reduction projects. Significantly higher rebound effects can be captured in developing economies, but they could be attenuated by government policies (Pollin, 2018);
- fossil fuel mix; the actual (2019) fuel mix and the equivalent emission factor in Italy based on Tables 1 and 2 is 463.6 $kgCO_{2,eq}$/MWh.
- renewable mix; resuming the data of Tables 3 and 5 the renewable equivalent emission factor in Italy accounts for 26.8 $kgCO_{2,eq}$/MWh.
- the data adopted for the intensity factors of fossil and renewable plants are the average of data shown in Table 4.
- the data assumed for the greenhouse emission per MWh of renewable conversion plants are the average of data shown in Table 3.
- it is assumed that these levels of emissions in 2050 could be reduced by 20%. This result could be obtained by a fuel mix redistribution[7] and the technology transition to combined power

[6] with the exception of periodic growth rate models lasting for 40 years.

[7] the decomposition analysis shows that historically the reduction of the equivalent CO_2 emissions of the thermoelectric plants is due to the increasing share of natural gas, which in turn has a positive effect on the electrical conversion efficiency of plants, (ISPRA, 2021b).

Table 5
Fossil fuel and renewable mix in Italy at T_0 time [%].

Type of fuels in fossil fuel plants	Electric energy generation share at T_0 (2019) [%]	Type of resource in renewable fuel plants	Electric energy generation share at T_0 (2019) [%]
Solid	9.6	Hydropower	47
Natural gas	72.5	Wind	21
Derived gas	1.2	PV	25
Oil products	5.2	Geothermal	6
Other fuels (no biomass)	11.3	Others	1

plants. The increase in the share of wind and solar energy conversion technology will lead to an equivalent drop in the renewable emission factor of 20%.

5.2. Limitations of the model

The limitations of the model are:

- the electric energy consumption, deduced from BP data (BP, 2020), corresponds to the user side, and not to the level of production side, since this should include the additional quote for energy dispatching. This quantity is country-specific, generally amounts to a few percent of the total, and is not considered in the model, but could be readily included in a country-specific study;
- the availability of renewable sources is based on: (i) the hypothesis of an endless availability of renewable resources, providing an infinite quantity of green fuel (water, wind, and sun intensity) to feed the conversion plants; some scenario of substitution is clearly incompatible with the renewable resource availability and accessibility of some countries. (ii) ignoring the commissioning time required to build new power conversion plants; this time lag could be not compatible with the marginal growth of the plants required to 'instantly' fulfil the energy demand, and becoming a displacing-limiting factor for renewable energies in the transition scenario; (iii) ignoring the contribution to total emission of any additional infrastructures commissioning/decommissioning and operation (i.e. electric lines and substations, storage plants, etc.) needed for the electric energy distribution;
- the role of biomass and CO_2 capture technology can play a role in the future to partially offset fossil fuel emissions, but, in the timeframe investigated, can only contribute marginally, due to the lack, to date, of technologically mature solutions. Their inclusion can be implemented or discarded without compromising the general model. As far as new CO_2 sequestration technology will be available, this option can be implemented as a suitable subtracting factor from the yearly GHG emission and from the final GHG inventory;

These limitations of the model result globally in an underestimation of the actual emission levels, which generates a best-scenario prediction.

5.3. Indicators

The indicators generated for the analysis are:

- the electric energy demand (covered by fossil and renewable sources);
- the ratio between renewable and fossil energy E_r/E_f; it represents the relative penetration rate of the intermittent sources.
- the power capacity;
- the ratio between the energy at year T and that at year zero T_0 $(E/E_{T0})_f$, $(E/E_{T0})_r$, and the relative power of the plants at year T and that at year zero T_0 $(P/P_{T0})_f$, $(P/P_{T0})_r$.
- the power capacity marginal growth factor (PMGF). As far as fossil fuel plants are concerned, the overall commissioning times (authorizations, project, construction) can vary between 5 and 12 years. These times for renewable source plants generally range between 2 and 4 years for solar and wind power plants, while they can take up to 10 years for basin hydroelectric plants;
- the value of the global equivalent $CO_{2,eq}$ or GHG produced and saved for each scenario.

Table 6 shows the list of simulations generated by the combination of the hypotheses and the models presented.

5.4. Energy and power results

The first block of simulations (#1, #2 and #3) refers to the future energy and power demand considering the partial replacement (substitution) over time of fossil sources by renewable ones (Er_{T_0} = 39.5% - $Er_{T_{30}}$ = 60.5%, Ef_{T_0} = 60.5% - $Ef_{T_{30}}$ = 39.5%) according to the three growth scenarios: low (2%), medium (4%), and high (7%). It is assumed that there are no improvements in the load factor of the plants. However, an attenuation of the energy intensity of the electricity consumption processes is considered. Figs. 8–9 indicate that the i = 2% scenario leads to global growth of energy demand and power of 175%. This scenario can be accomplished by strong growth of renewable energy and power (+280%), and moderate growth (+20%) in the electricity produced with fossil sources. Accordingly, the power capacity from fossil fuels over the next 30 years rises marginally, and this implies (see Fig. 9) a slow decrease in the installation ratio (with a drop from 1% to 0%) excluding the rate of plant replacement due to obsolescence at the end of their technical life and a consistent rise of installation of renewable plants (from 4% to 3% in the period).

Both the i = 4% and i = 7% scenarios imply significant increases in the energy required and the power installed (see Figs. 10–11, Figs. 12–13). The power produced by fossil plants needs to increase by more than 200% for a growth rate of 4%, and by over 500% for the 7% scenario. Although the marginal installed capacity of fossil fuel plants slows slightly yearly, the plant's installation rate remains very high, over 6% for i = 7% (see Fig. 13). The installation ratio of the renewable fuelled plants is even higher, close to 10% for the most demanding scenario, making it very difficult to find new candidate sites. The energy penetration of renewable energy achieves parity into the grid with fossil one after 15 years regardless of the growth rate, due to the linear (top to bottom) penetration law. The second block of simulations (#4, # 5, and #6) refers to a situation of energy demand and future power similar to the previous simulations, but where the renewable penetration target will achieve 90% from a renewable source (complete penetration) through a linear substitution pattern. Figs. 14–15, Figs. 16–17, Figs. 18–19 help in assessing the three scenarios of low, medium, and high growth. The trend towards complete penetration seems to attenuate the growth rate of energy and power from fossil sources for the low scenario, which will consequently lead to a marked uninstallation rate of fossil-fuelled plants over the years. The increase in fossil power doubles in the high-growth scenario. Nevertheless, the low growth scenario allows an immediate and progressive decommissioning rate of fossil fuelled plants. For medium and high scenarios this condition is shifted at year t=10, and$t$ = 20 respectively. There is a considerable increase in the exploitation of renewable sources from 400% (at i = 2%) to 800% (at i = 4%) up to more than 1800% (at i = 7%). As the renewable plant installation rate is high, these scenarios entail massive resource scouting (wind, hydraulic, solar), selecting technologies, finding suitable geographical areas, and selecting the infrastructures to dispatch the electrical energy. It is also clear that even in the slowest growth scenario (i = 2%), well before the first decade, the quantity of electricity produced from renewable sources exceeds that of fossil sources, with the need to develop infrastructures capable of managing intermittent flows with an ever-decreasing regulating capacity of the fossil rotating

Table 6
List of the simulations generated by the combination of the hypotheses and the models presented.

SIM. #	Growth law	Growth rate	Renewable sources penetration law	Attenuation model	LF fossil fuelled plants [–]	LF Renewable fuelled plants [–]
1	$f(i) = e^{iT}$	i = 2% constant	linear 39.5%→60.5%	a_f = 2%	33% constant	20% constant
2	$f(i) = e^{iT}$	i = 4% constant	linear 39.5%→60.5%	a_f = 2%	33% constant	20% constant
3	$f(i) = e^{iT}$	i = 7% constant	linear 39.5%→60.5%	a_f = 2%	33% constant	20% constant
4	$f(i) = e^{iT}$	i = 2% constant	linear 39.5%→90%	a_f = 2%	33% constant	20% constant
5	$f(i) = e^{iT}$	i = 4% constant	linear 39,5%→90%	a_f = 2%	33% constant	20% constant
6	$f(i) = e^{iT}$	i = 7% constant	linear 39.5%→90%	a_f = 2%	33% constant	20% constant
7	$f(i) = e^{iT}$	i = 2% constant	logistic 39.5%→90%	a_f = 2%	33% constant	20% constant
8	$f(i) = e^{iT}$	i = 4% constant	logistic 39.5%→90%	a_f = 2%	33% constant	20% constant
9	$f(i) = e^{iT}$	i = 7% constant	logistic 39.5%→90%	a_f = 2%	33% constant	20% constant
10	$f(i) = e^{iT}$	i = 2% constant	logistic 39.5%→90%	a_f = 2%	33%→45% linear	20%→25% linear
11	$f(i) = e^{iT}$	i = 4% constant	logistic 39.5%→90%	a_f = 2%	33%→45% linear	20%→25% linear
12	$f(i) = e^{iT}$	i = 7% constant	logistic 39.5%→90%	a_f = 2%	33%→45% linear	20%→25% linear
13	$f(i) = 0.02(1 + sin(\pi/2 \cdot T/5))$	periodic	logistic 39.5%→90%	a_f = 2%	33% constant	20% constant
14	$f(i) = 0.02(k \cdot T + sin(\pi/2 \cdot T/5))$	periodic increasing	logistic 39.5%→90%	a_f = 2%	33% constant	20% constant
15	$f(i) = 0.02 - 0.01e^{(-0.1iT)}$	increasing attenuated	logistic 39.5%→90%	a_f = 2%	33%→45% linear	20%→25% linear
16	$f(i) = 0.04e^{-(0.5 \cdot 0.04T)}$	4% → 2%	logistic 39.5%→90%	a_f = 2%	33% → 45% linear	20%→25% linear
17	$f(i) = 0.04e^{-(2.0 \cdot 0.04T)}$	4% → ∼0%	logistic 39.5%→90%	a_f = 2%	33% → 45% linear	20%→25% linear

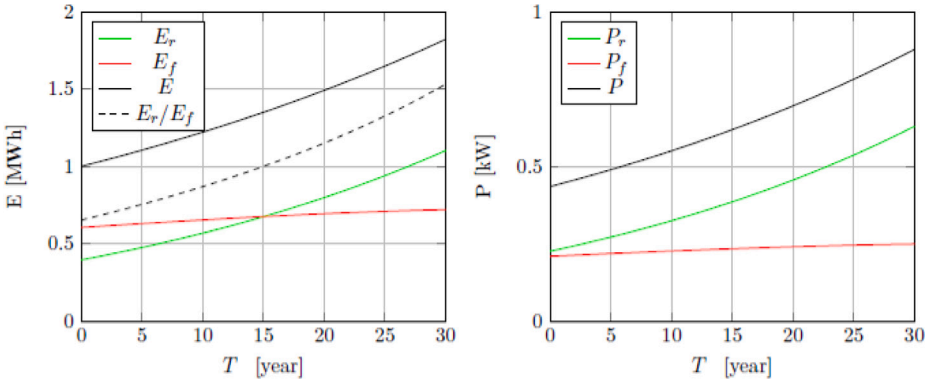

Fig. 8. Simulation #1 - fossil and renewable electrical energy (left) and power (right) demand trend.

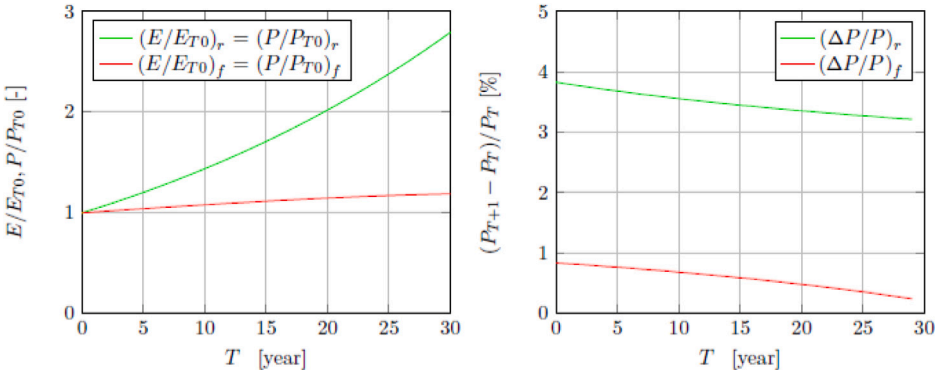

Fig. 9. Simulation #1 - ratios of electricity and power demand from fossil and from renewable sources (left), and marginal ratios of energy and power (right).

part. This means that part of the progressive decommissioning of fossil fuel plants should become part of the rotating reserve, and cannot be dismissed.

The third block of simulations (#7, #8, and #9) shows the results of the logistic penetration law of renewable sources, with the goal to achieve, at the end of the period, a generation target based on 90% from renewable sources and 10% from fossil sources. The logistic penetration model is characterized by the typical convergence of the renewable and fossil marginal power, as shown in the last plot of each figure group 20–21, 22–23, 24–25. In the i = 2% and i = 4% scenarios, the energy produced from fossil sources decreases and asymptotically forms a plateau after 15 years, with a small increase in the last decade of the time frame. Decommissioning of fossil-fuelled plants is readily possible for low and medium scenarios, but refiring at year$t$ = 20 when the transition model shows a slowing down of renewable yearly contribution becomes necessary already for the medium growth scenario. On the other hand, in the high development scenario, the contribution of fossil sources to the energy system again becomes necessary in the second decade to satisfy the high energy demand. The decelerating trend caused by the logistic penetration of renewables

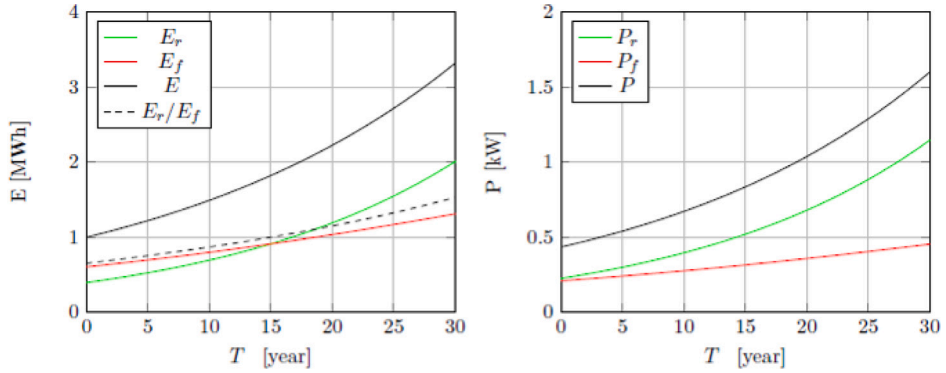

Fig. 10. Simulation #2 - fossil and renewable electrical energy (left) and power (right) demand trend.

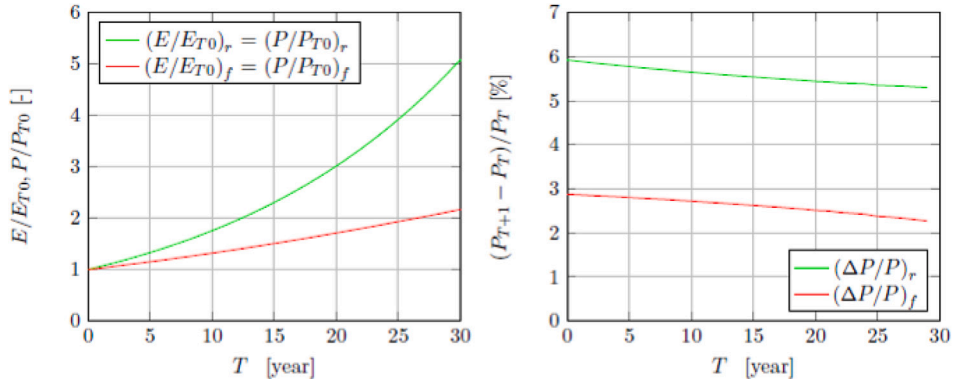

Fig. 11. Simulation #2 - ratios of electricity and power demand from fossil and from renewable sources (left), and marginal ratios of energy and power (right).

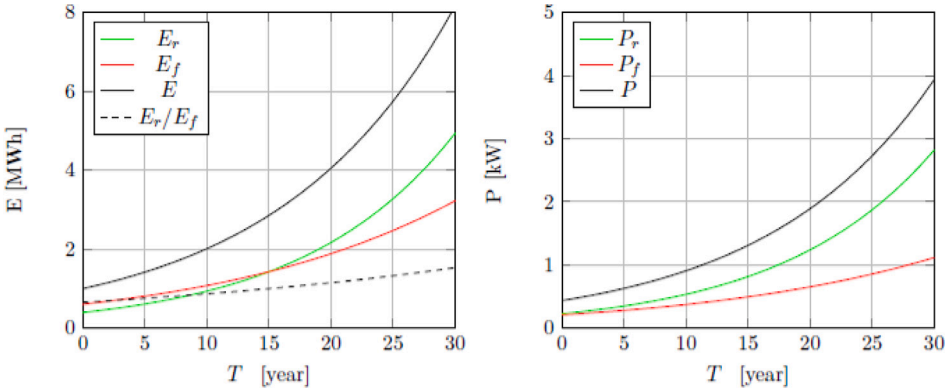

Fig. 12. Simulation #3 - fossil and renewable electrical energy (left) and power (right) demand trend.

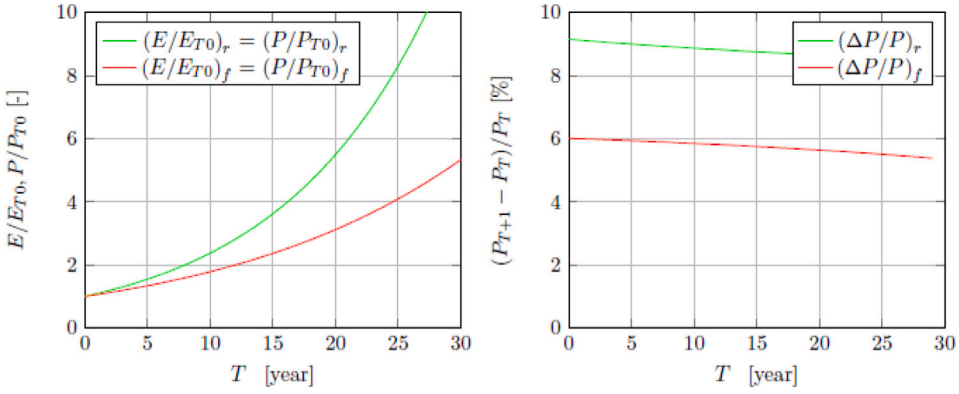

Fig. 13. Simulation #3 - ratios of electricity and power demand from fossil and from renewable sources (left), and marginal ratios of energy and power (right).

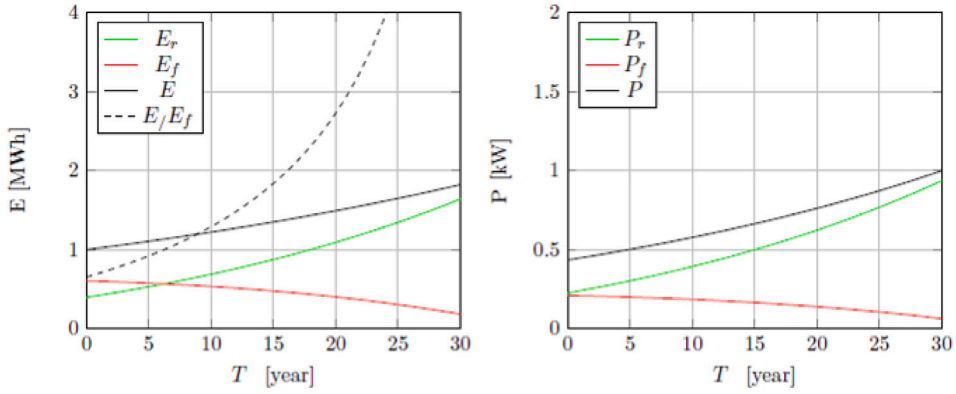

Fig. 14. Simulation #4 - fossil and renewable electrical energy (left) and power (right) demand trend.

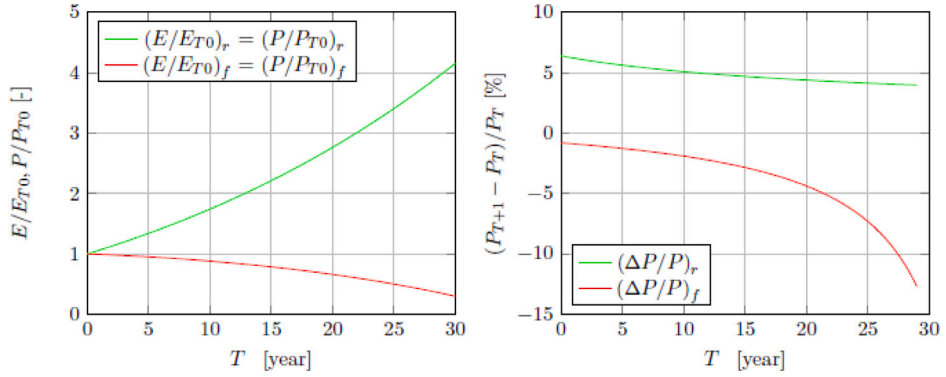

Fig. 15. Simulation #4 - ratios of electricity and power demand from fossil and from renewable sources (left), and marginal ratios of energy and power (right).

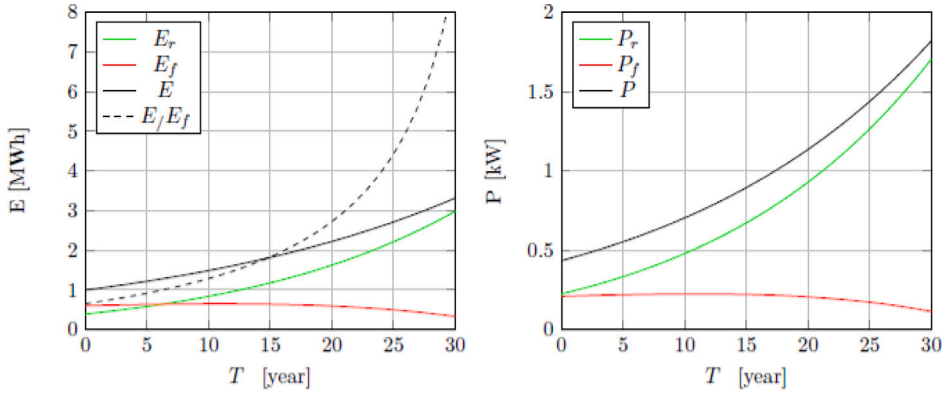

Fig. 16. Simulation #5 - fossil and renewable electrical energy (left) and power (right) demand trend.

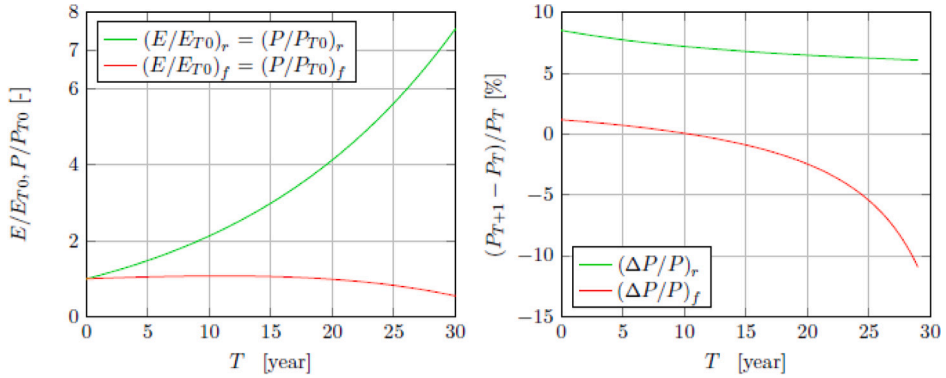

Fig. 17. Simulation #5 - ratios of electricity and power demand from fossil and from renewable sources (left), and marginal ratios of energy and power (right).

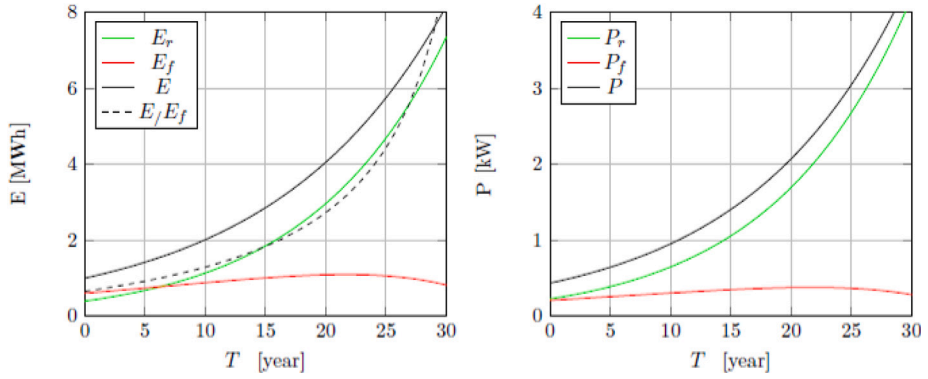

Fig. 18. Simulation #6 - fossil and renewable electrical energy (left) and power (right) demand trend.

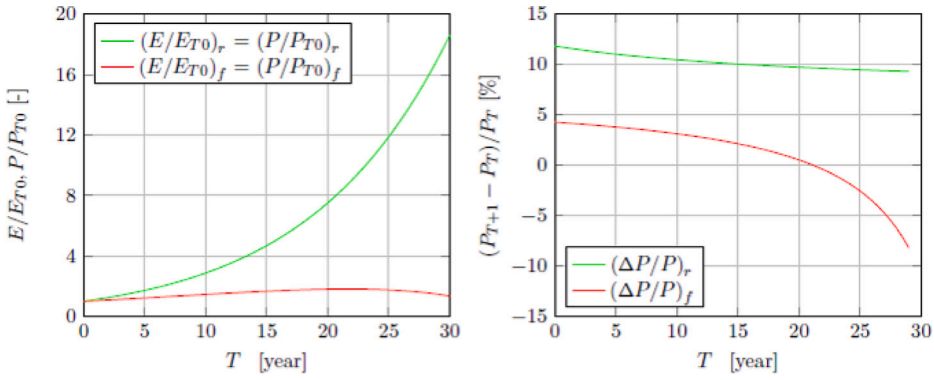

Fig. 19. Simulation #6 - ratios of electricity and power demand from fossil and from renewable sources (left), and marginal ratios of energy and power (right).

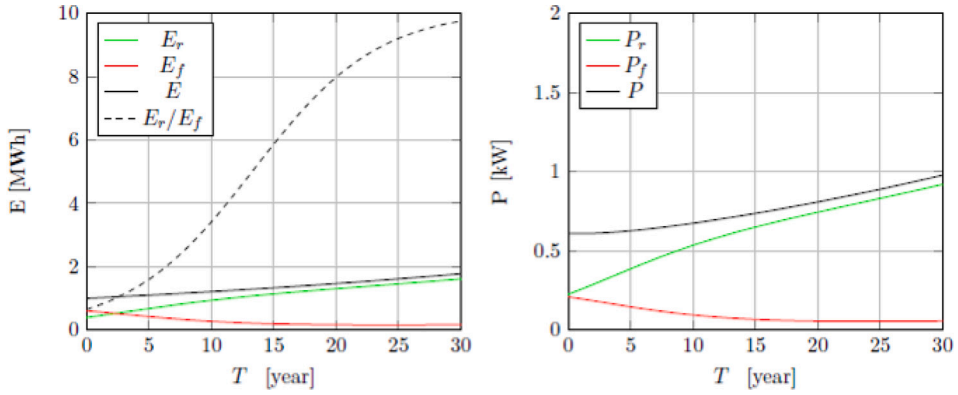

Fig. 20. Fossil and renewable electrical energy (left) and power (right) demand trend.

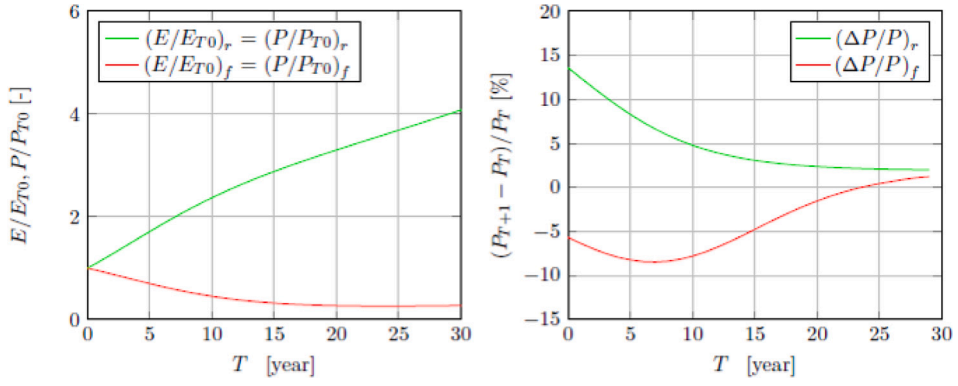

Fig. 21. Ratios of electricity and power demand from fossil and from renewable sources (left), and marginal ratios of energy and power (right).

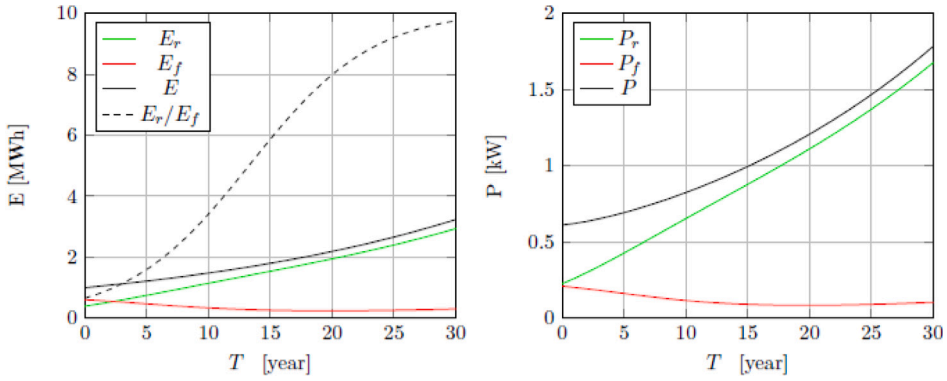

Fig. 22. Fossil and renewable electrical energy (left) and power (right) demand trend.

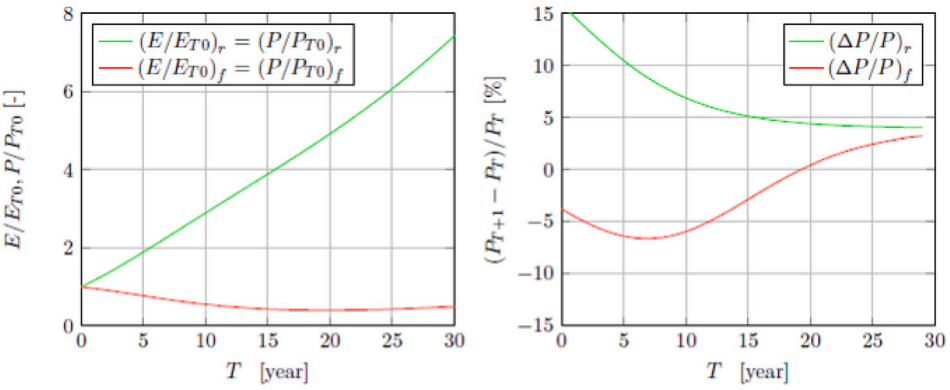

Fig. 23. Ratios of electricity and power demand from fossil and from renewable sources (left), and marginal ratios of energy and power (right).

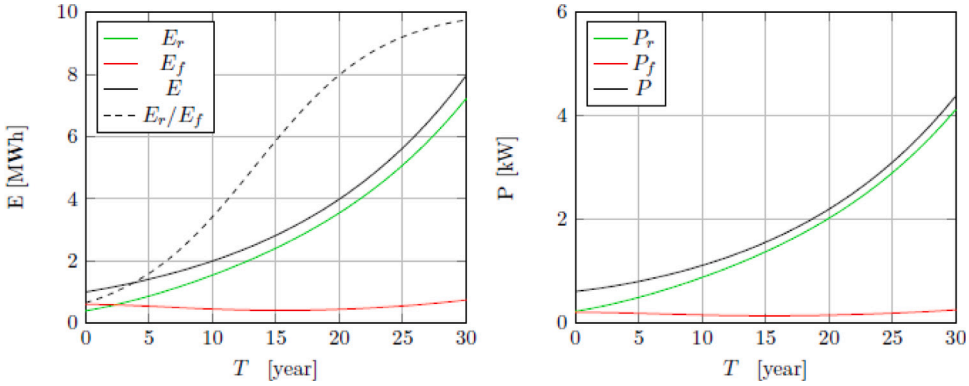

Fig. 24. Fossil and renewable electrical energy (left) and power (right) demand trend.

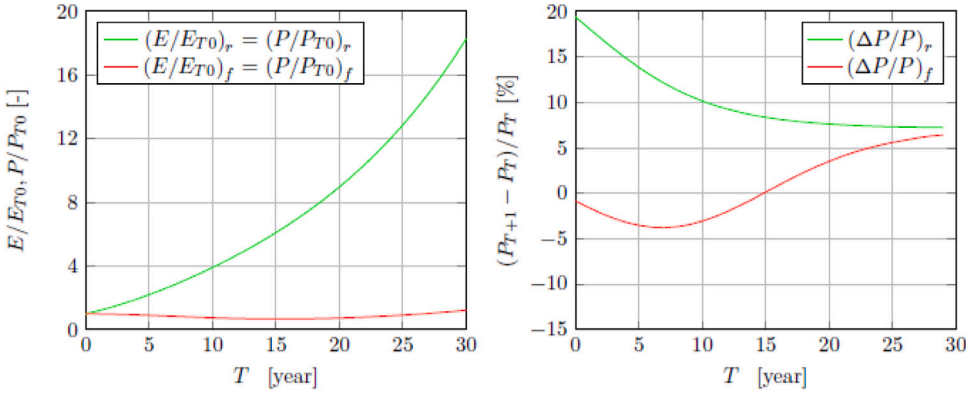

Fig. 25. Ratios of electricity and power demand from fossil and from renewable sources (left), and marginal ratios of energy and power (right).

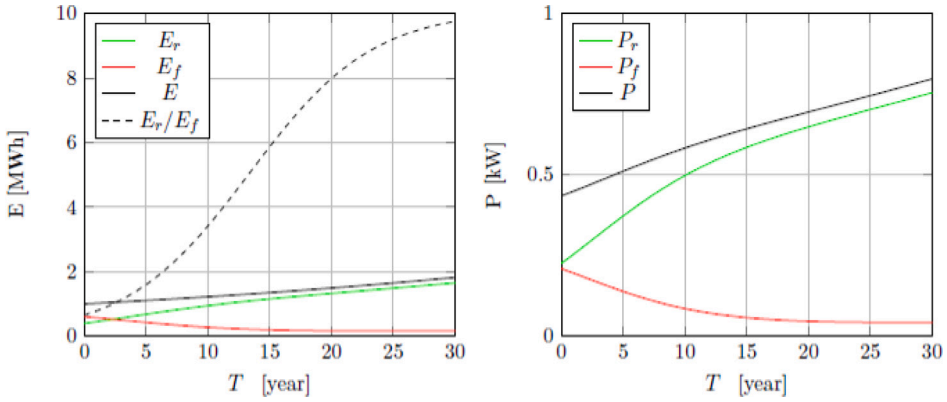

Fig. 26. Fossil and renewable electrical energy (left) and power (right) demand trend.

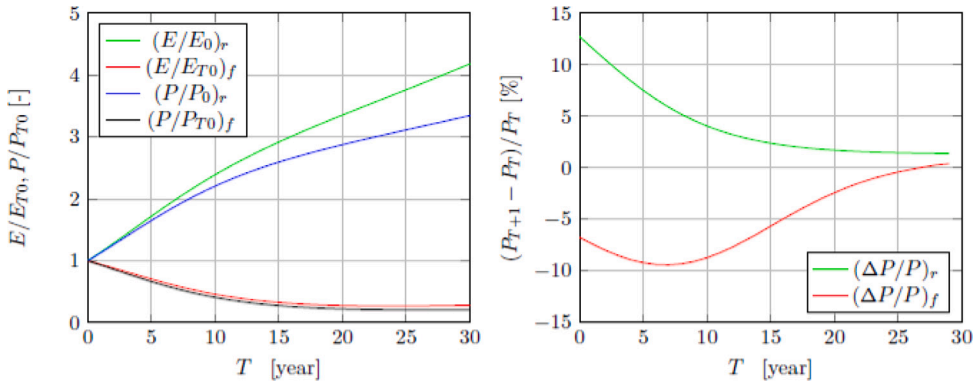

Fig. 27. Ratios of electricity and power demand from fossil and from renewable sources (left), and marginal ratios of energy and power (right).

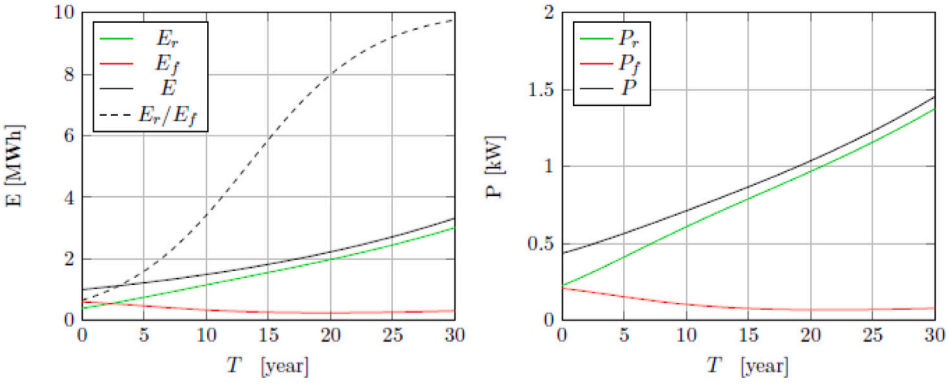

Fig. 28. Fossil and renewable electrical energy (left) and power (right) demand trend.

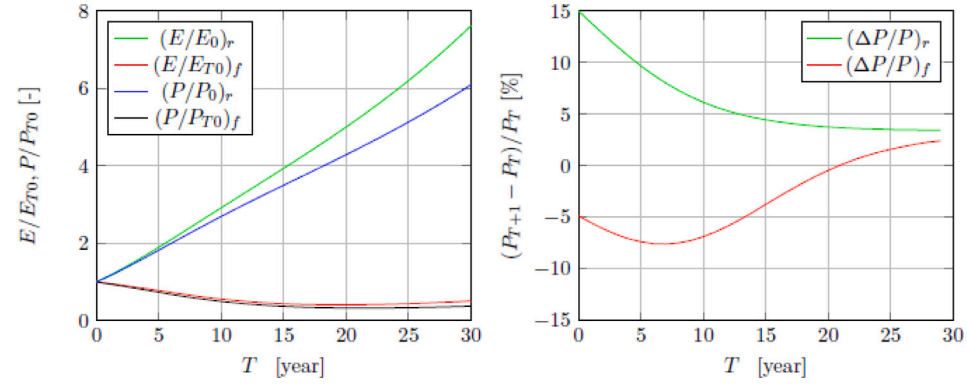

Fig. 29. Ratios of electricity and power demand from fossil and from renewable sources (left), and marginal ratios of energy and power (right).

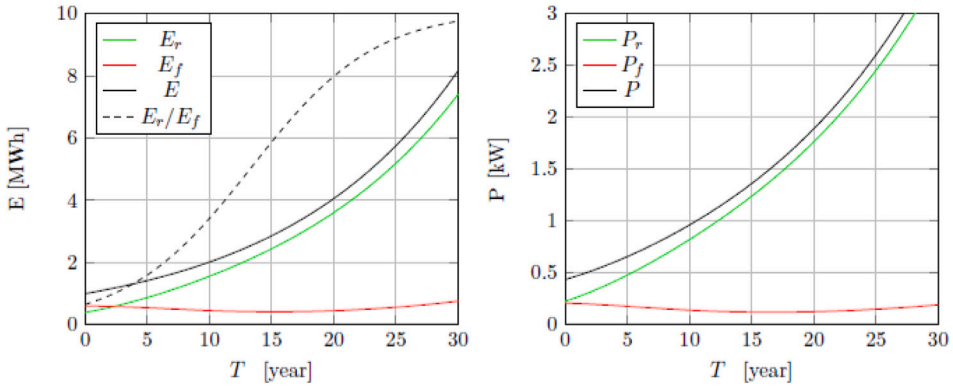

Fig. 30. Fossil and renewable electrical energy (left) and power (right) demand trend.

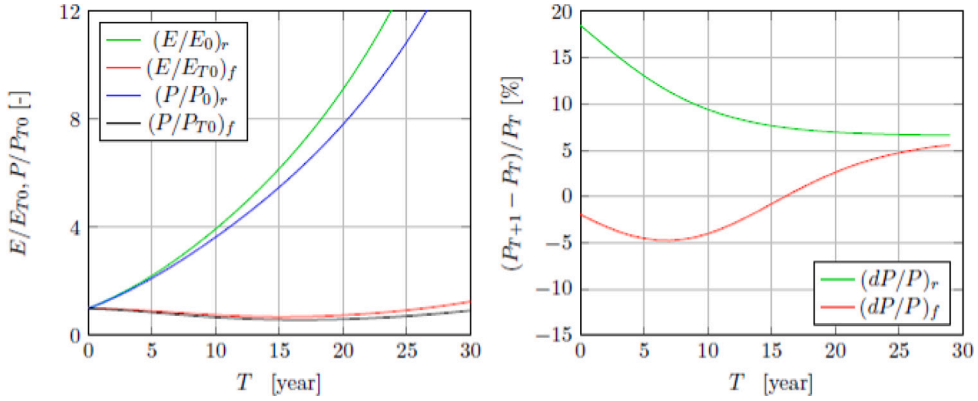

Fig. 31. Ratios of electricity and power demand from fossil and from renewable sources (left), and marginal ratios of energy and power (right).

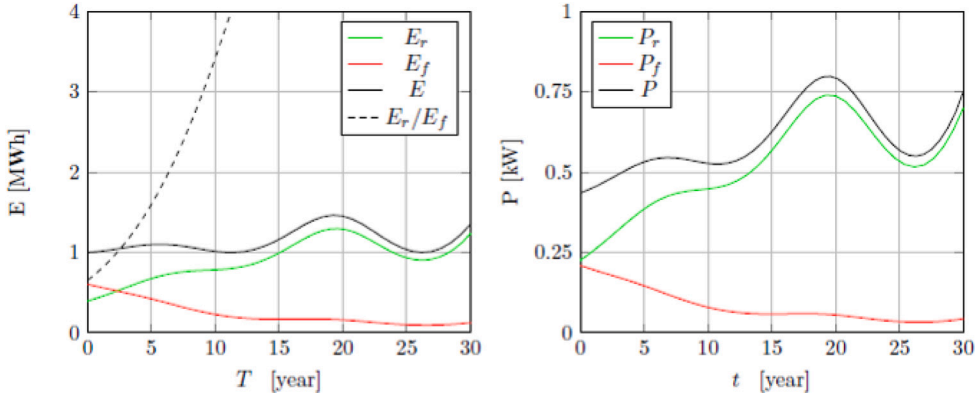

Fig. 32. Fossil and renewable electrical energy (left) and power (right) demand trend.

leads to a decreasing marginal installation rate of renewable plants, which stabilizes to a constant plant capacity installation ratio halfway through the period, while the number of fossil plants rapidly increases. Only the $i = 2\%$ scenario leads to a near zero renewable installation rate at the end of the period.

The fourth block of simulations (#10, #11, and #12) is similar to the previous block but adds the effect of technological advances through the increase in the plant's load factor: $LF = 33\% \rightarrow 45\%$ for fossil fuel plants and $LF = 20\% \rightarrow 25\%$ for renewable energy plants. Figs. 26–27, 28–29, 30–31 show that the main benefit is that the same requirement of total energy is obtained with less plant capacity (−25%), either renewable or fossil, which is important especially to reduce the fossil contribution to the total. The high-demand scenario is still critical, as it requires the contribution of new fossil plants after 15 years. On the other hand, in the low growth scenario both stabilize to about zero annual rates, this common rate tend to be about 2.5%, and about 5% for the medium and high scenarios respectively. The E_r to E_f parity is achieved within about six years.

The scenario of simulation #13 (Figs. 32–33) indicating a periodic energy demand fluctuation around a long average growth rate of $i = 1\%$, leads to a complex path with oscillations in the energy and power requirements. With regard to marginal power trends, steep gradients emerge, making the planning phase of construction and management of the plants complex. Globally this scenario reduces the supply of fossil fuel energy, but small oscillations will be dramatically amplified.

The situation of the periodic but increasing trend over time (simulation #14 - (Figs. 34–35) is similar to the case of simulation #13, and requires no further comments.

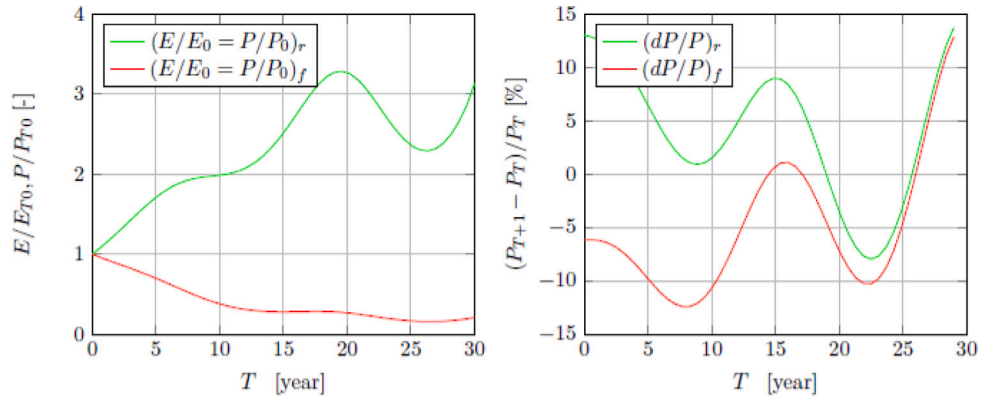

Fig. 33. Ratios of electricity and power demand from fossil and from renewable sources (left), and marginal ratios of energy and power (right).

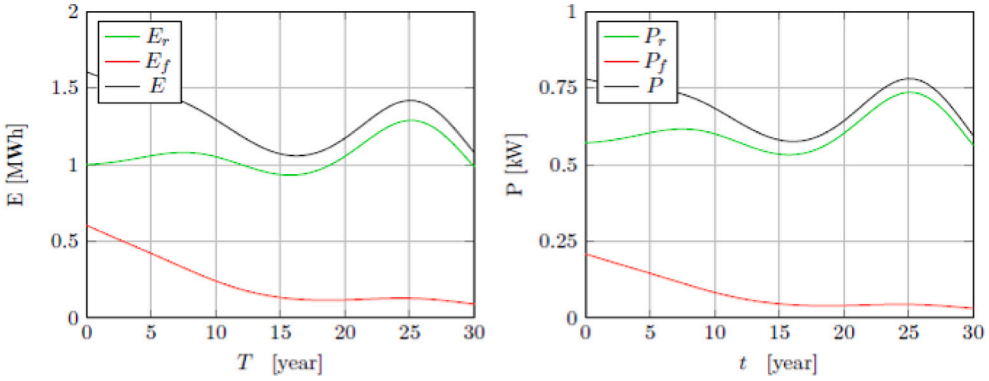

Fig. 34. Fossil and renewable electrical energy (left) and power (right) demand trend.

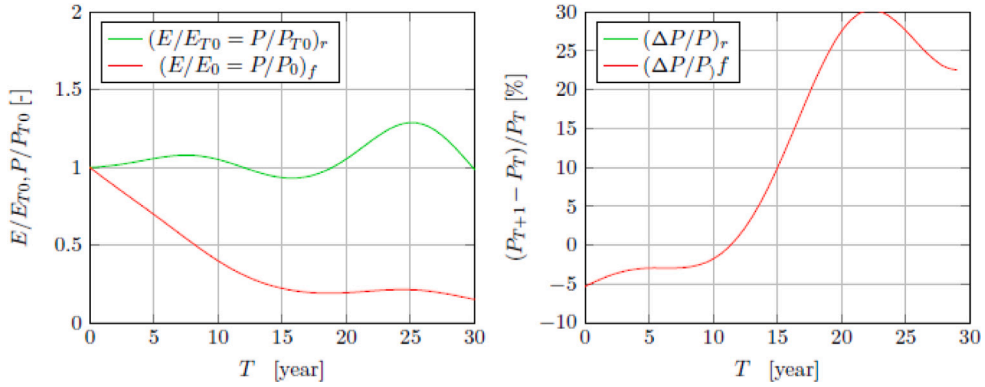

Fig. 35. Ratios of electricity and power demand from fossil and from renewable sources (left), and marginal ratios of energy and power (right).

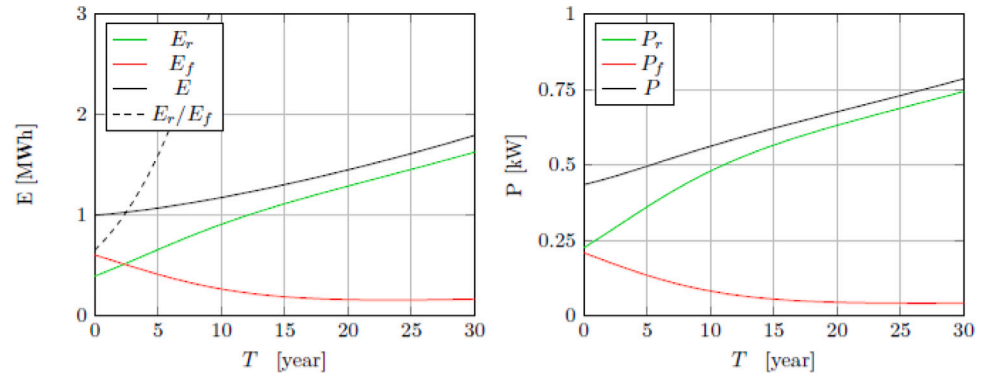

Fig. 36. Fossil and renewable electrical energy (left) and power (right) demand trend.

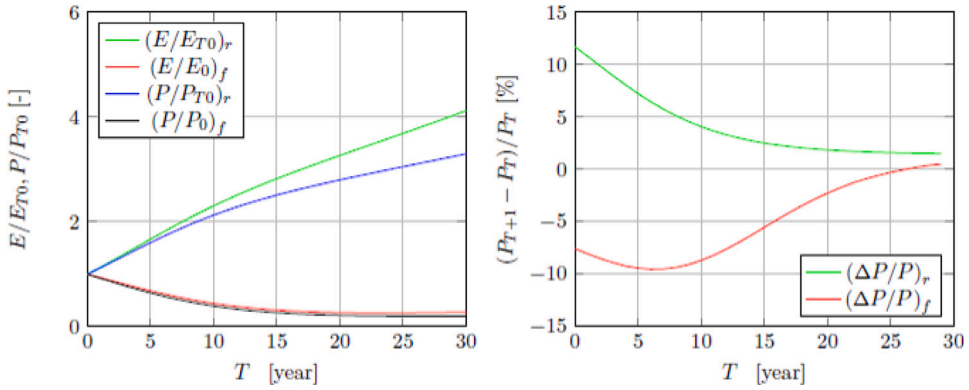

Fig. 37. Ratios of electricity and power demand from fossil and from renewable sources (left), and marginal ratios of energy and power (right).

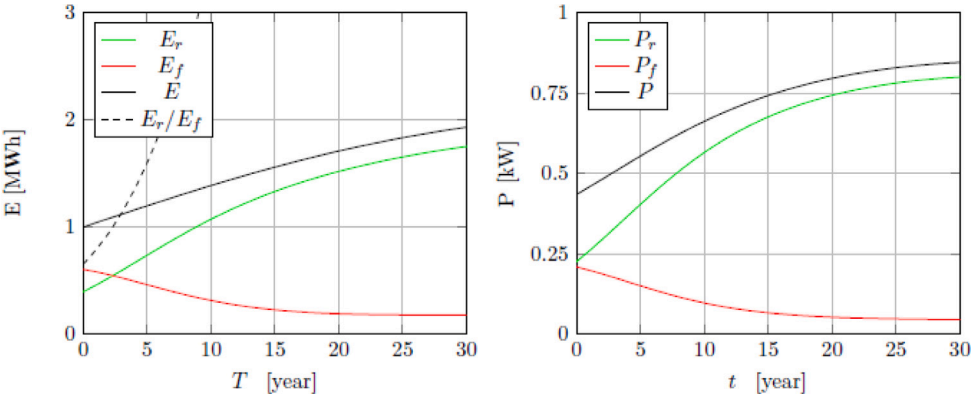

Fig. 38. Fossil and renewable electrical energy (left) and power (right) demand trend.

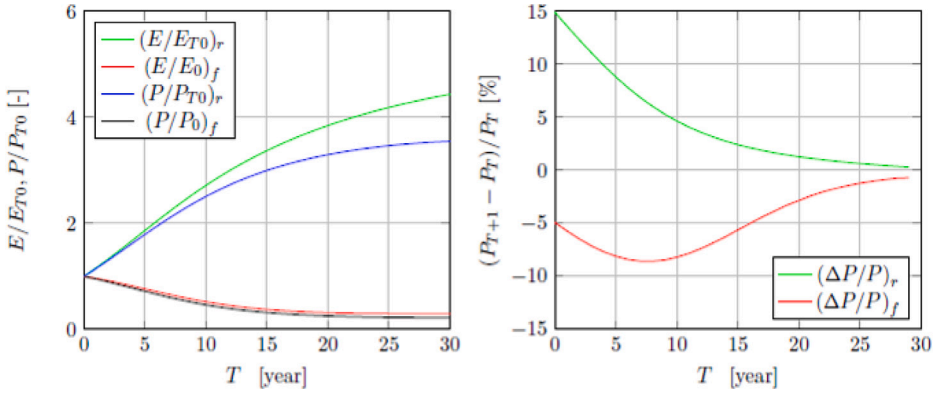

Fig. 39. Ratios of electricity and power demand from fossil and from renewable sources (left), and marginal ratios of energy and power (right).

Simulation #15 through Figs. 36–37 shows the case of an attenuated growth from $i = 1\%$ to $i = 2\%$. The energy indicates an escalating growth, but with a decreasing rate in fossil contribution. This trend reflects a reduction in the fossil power contribution, which is reduced to a quarter, while the renewable power plant capacity grows by more than 300%. The saturation of renewables leads to a downward trend and reaches a constant installation rate at the end of the period, while fossil plants decommissioning slows down.

The simulation #16 refers to the degrowth scenario and replacement of fossil fuels. The situation of the constant decrease rate with linear substitution, from $i = 4\%$ to $i = 2\%$ under a logistic transition rate: (39,5% to 90%) is shown in Figs. 38–39, leading to an increase in the demand for total energy (+200% in thirty years). At the same time, there is a reduction in the fossil contribution, accompanied by a reduction in the capacity at a very high ratio in the first years, followed by a less intense but moderate decrease. The effect of the degrowth is also reflected in the growth rate of renewable source plants which also undergo a reduction in the installation ratio after the first twenty years, followed by a near-zero rate, while the fossil plants start immediately with a strong decommissioning rate, which attenuates at the end of the period. Although considerably less, the fraction of power produced by fossil fuel plants remains constant after the first half of the period, and cannot be reduced further.

Figs. 40–41 report the situation of case #17, where the growth rate falls to nearly zero, taking full advantage of technology advancements (growing LFs). This scenario indicates that the total energy demand

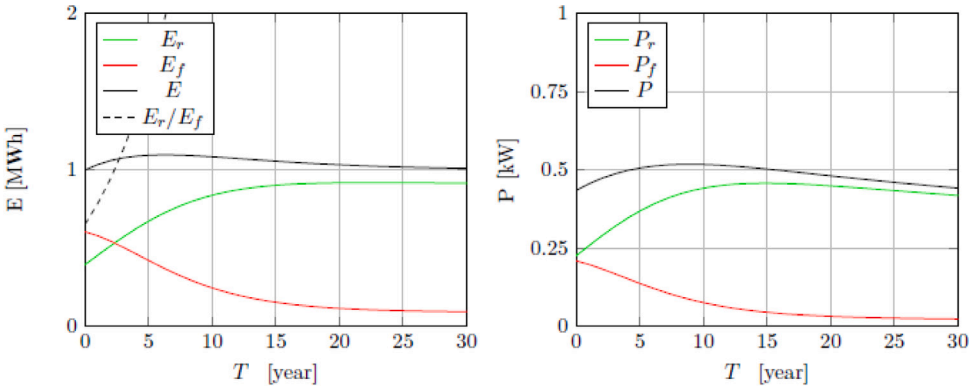

Fig. 40. Fossil and renewable electrical energy (left) and power (right) demand trend.

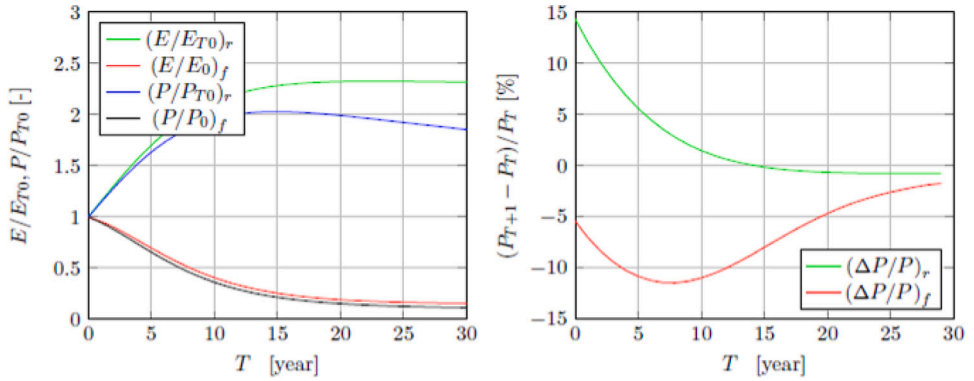

Fig. 41. Ratios of electricity and power demand from fossil and from renewable sources (left), and marginal ratios of energy and power (right).

remains slightly decline over the period of observation, like the power capacity. The electric energy produced by fossil fuels achieves a minimum stabilized at about 10% of the initial share. The renewable energy share decreases too at the end of the period and after about 15 years plants can be decommissioned.

5.5. GHG emissions results

According to the GHG emission model and the hypothesis made, renewable energies are expected to primarily play the role of avoiding future emissions, while their contribution to GHG production remains small, even in the highest energy-demanding scenario.

The plots indicate the GHG emissions [kg] emitted yearly as a function of the electrical energy produced/consumed according to the most interesting scenarios analysed in Table 6. As the energy quantity at year T_0 has been set at 1 MWh, the emissions of one specific year can be computed by multiplying the data plotted by the actual electrical energy produced. The graph, in the boxes placed at the end of the period, shows the total inventory of GHG emitted in the entire period. The actual total GHG emitted can thus be obtained by multiplying this data by the total energy produced at the end of the period. Scenarios #4, #5, and #6 (Fig. 42) consider the low, medium and high growth rates ($i = 2\%$, $i = 4\%$ and $i = 7\%$) under a linear renewable penetration (90% at $t = T_{30}$), under the condition of a linear fossil greenhouse gas drop rate: $GHG_{2020} = 462.2$ kg/kWh $\rightarrow$ $GHG_{2050} = 0.8 \cdot GHG_{2020} kg$/kWh, as well as a linear renewable greenhouse gas drop rate: $GHG_{2020} = 26.3$ kg/kWh $\rightarrow$ $GHG_{2050} = 0.8 \cdot GHG_{2020} kg$/kWh. The scenarios lead to a drop of about 40% of the GHG emissions over the period considered. The total GHGs emitted are 11.8 kg for $i = 2\%$, and 13.5 kg for $i = 4\%$. The high growth scenario ($i = 7\%$) ends with almost the same emissions recorded at $t = T_0$, but the trend increases in the first 20 years, to decrease after. The total GHGs emitted in the period, therefore, amount to 17.7 kg. Renewable plants, in this scenario, avoid about 26 kg, while in the low to medium scenario, the contribution becomes less and less important. Nevertheless, these saved emissions are not sufficient to offset or satisfactorily reduce the emissions caused by the energy demand.

Compared to the previous scenario, the logistic penetration law shown in Fig. 43 for simulations #7, #8, and #9, produces a faster decline in the GHG emissions, with greater avoidance of GHGs compared to the linear penetration case. The decrease is about 54% for the low scenario and about 40% for the medium growth rate scenario, with a consistent flattening of the yearly emissions. There is an initial half-period decrease in the booming consumption in the high growth rate scenario followed by a rise in GHGs until the end of the period. The logistic penetration case seems to be more benign than the linear one, with a dramatic global damping of emissions avoided thanks to renewables of 30 kg, and a marked contribution for the other cases.

The fluctuating demand (Fig. 44) over 15 years in scenario #13 creates a very fast decrease in GHGs in the first half of the period, followed by a waved plateau of fossil fuels emissions, where the contribution of renewables avoids about 80% of future emissions.

When the demand is still fluctuating but the general trend of consumption decreases (see case #14), for instance, due to long-term strategies of containment of the energy demand, the situation depicted in Fig. 45 is generated. The effect of a decrease in demand is reflected in a smoothing down of the emission curve after the first 15 years, and the emissions avoided amount to about half of the total emissions at the end of the period.

The emissions associated with the attenuated growth case from $i = 1\%$ to 2% (case #15 and Fig. 46) show a drop of about 40% up to

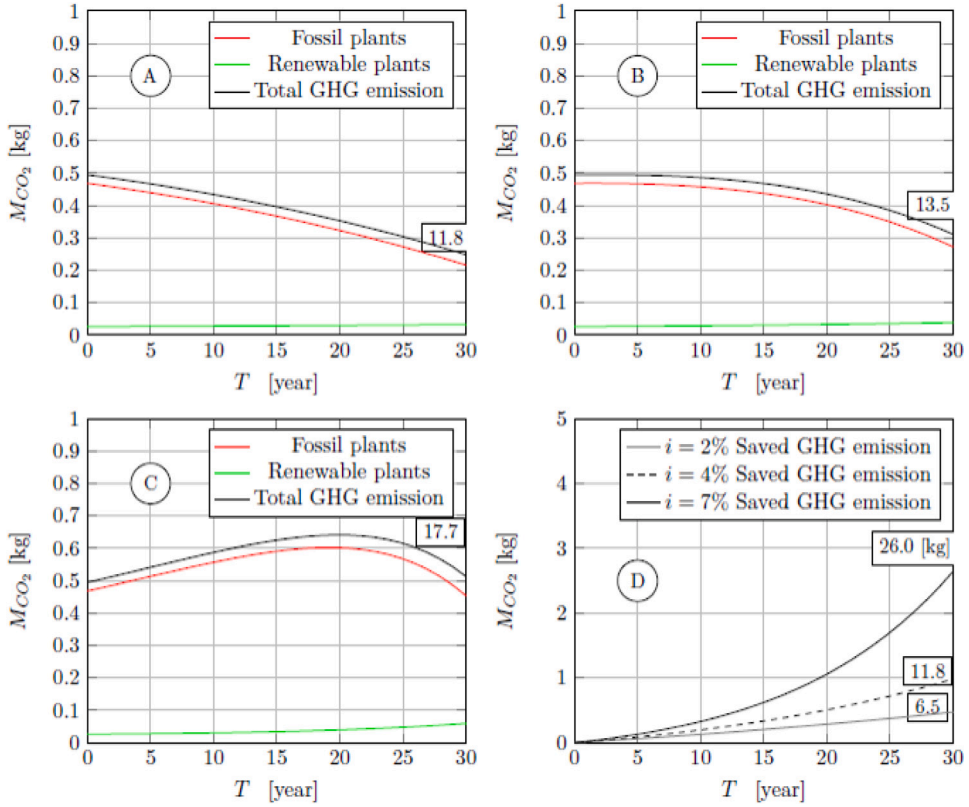

Fig. 42. GHG emission: Scenarios #4, #5, and #6: (A) - $i = 2\%$, (B) - $i = 4\%$, (C) - $i = 7\%$, (D) - saved emissions. Boxed data indicate total GHG emissions [kg] of the whole period.

halfway through the period, after which the fossil emissions stabilize and start to increase in the second half.

Scenario #16 foreseeing a decrease rate from $i = 4\%$ to 2% (Fig. 47) indicates a trend of the continuous decline of emissions, with a threshold plateau in the reduction of GHG emissions of about 50%. This case leads to a maximum reduction in emissions thanks to renewables of 10.4 kg, about the same as the total emissions of the period. Finally, the ideal exercise involving the full de-growth scenario of case #17 is provided in Fig. 48, where a hypothetical drop from $i = 4\%$ to $i = 0.5\%$ in thirty years is forecast. Again, no more than a 56% reduction in emissions is obtained and the total inventory of GHG emissions remains slightly above 9 kg. The trend indicates a sloping decrease after a mid-period, given by the saturated contribution of renewables, which shows the limit of green transition benefits in the field of electric energy demand.

6. Sensitivity analysis and method testing

A sensitivity analysis (Helton et al., 2006) was carried out to investigate how variations in the model input can qualitatively or quantitatively affect some output parameters (power, GHG, etc.). The input parameters considered are:

- the initial electric energy share $\left(E_r/E_f\right)_{T0}$; this parameter differs from country to country, and depends on the actual level of penetration of renewable energies at time $t = T_0$. This affects the GHG trend and the final GHG inventory at time $t = T_{30}$;
- the final electric energy share $\left(E_r/E_f\right)_{T30}$; this parameter can vary according to the penetration/substitution target set by an individual country at time $t = T_{30}$. This affects the GHG trend and the final GHG inventory at time $t = T_{30}$;
- the load factors $(LF)_r, (LF)_f$; the uncertainty regarding the load factor variation in the future has an impact on the power capacity, thus on $(P/P_{T0})_r$, and $(P/P_{T0})_f$. It depends on climate conditions, fuel availability, technology improvements, choice of conversion technology, etc.;
- the initial fossil emission factor $f_{f,T0}$; this impacts the GHG trend and the final GHG inventory at time $t = T_{30}$;
- the fossil emission factor variation $f_f = f(t)$ over the years; this impacts the GHG trend and the final GHG inventory at time $t = T_{30}$. The variation depends on the evolution of the fuel mix, which in turn depends on the future fuel supply strategy and general country options in energy plans.

Fig. 49 shows the effect of the initial renewable to fossil penetration share ($\left(E_r/E_f\right)_{T0}$) on GHG emissions in the period, compared to the baseline case $(E_r/E_f)_{T0}$=2:3, all other data constant. The trend of $GHG/GHG_{baseline}$ is always increasing for values of the initial $\left(E_r/E_f\right)$ share higher than 1:1. The worst scenario, in terms of global emissions, is situations where the production of energy due to renewable sources prevails at $t = T_0$ over fossil production (3:1). This is caused by the lower margin of exploitation of renewable energy in an energy-growing context. On the other hand, a situation characterized by a relatively ample margin for renewable growth (1:3) will lead to a drop of about 17% at the end of the period of GHGs compared to the baseline case.

With regard to the ratio between renewable to fossil energy generation at the end of the period ($\left(E_r/E_f\right)_{T30}$), Fig. 50 indicates that all scenarios will lead to an increase in GHG emissions, compared to the renewable full penetration rate (9:1), even if a 3:1 ratio will limit the global emissions at the end of the period to 13.5 kg, compared to the baseline of 10.4 kg.

Fig. 51 indicates, for the constant growth rate $i = 4\%$ case, the fossil plant fuelled capacity variation for different evolutions of the future fossil plant load factor, compared to the baseline condition $LF_{f,baseline} = 33 \rightarrow 45\%$. As expected, while the constant LF scenario produces a continuous increase in power installed, any technological

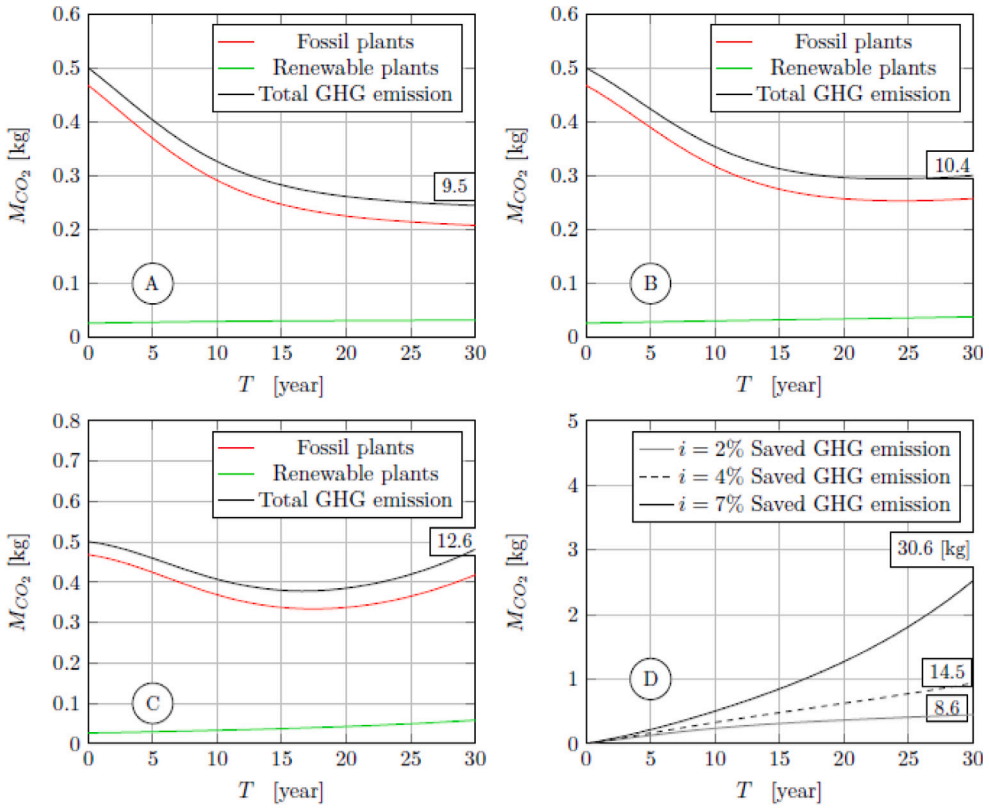

Fig. 43. GHG emission: Scenarios #7, #8, and #9: (A) - $i = 2\%$, (B) - $i = 4\%$, (C) - $i = 7\%$, (D) - saved emissions. Boxed data indicate total GHG emissions [kg] of the whole period.

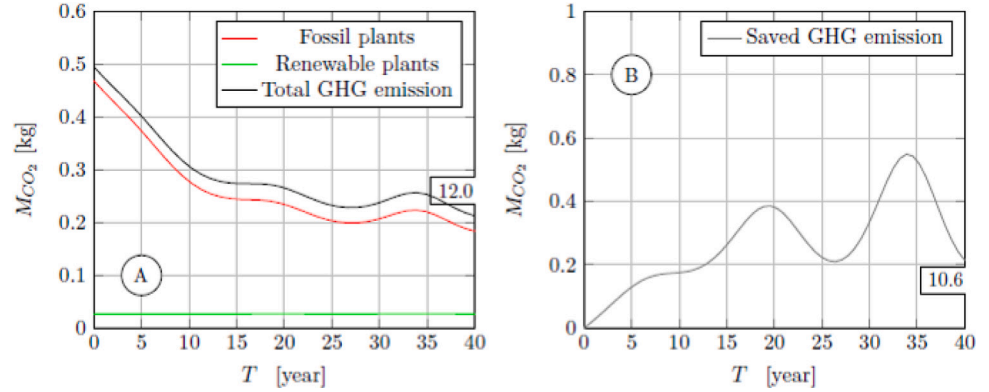

Fig. 44. GHG emission, scenario #13: periodic growth rate $i_{min} = 0\%$, $i_{max} = 2\%$ (period: 15 years).

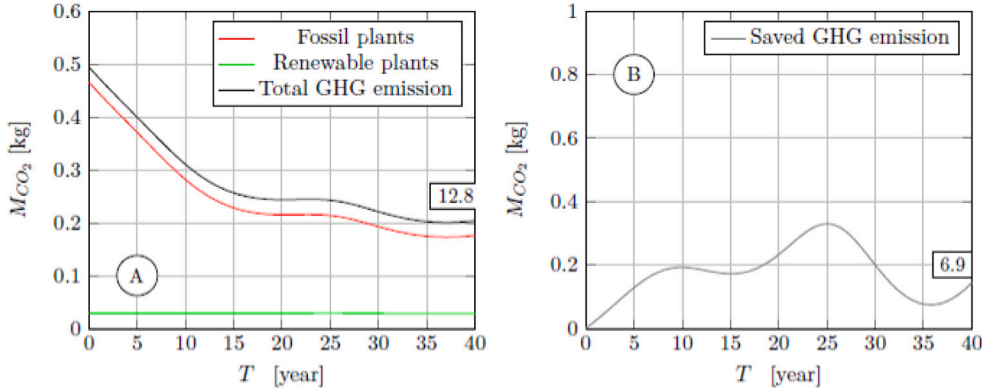

Fig. 45. GHG emissions, scenario #14: periodic growth rate $i_{min} = 0\%$, $i_{max} = 2.5\%$.

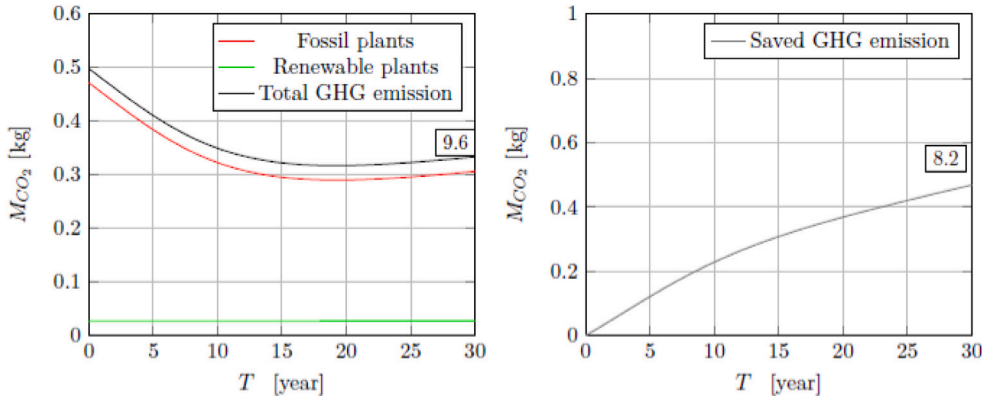

Fig. 46. GHG emission, scenario #15: attenuation growth rate: from $i = 1\%$ to $i = 2\%$. Boxed data indicate total GHG emissions [kg] of the whole period.

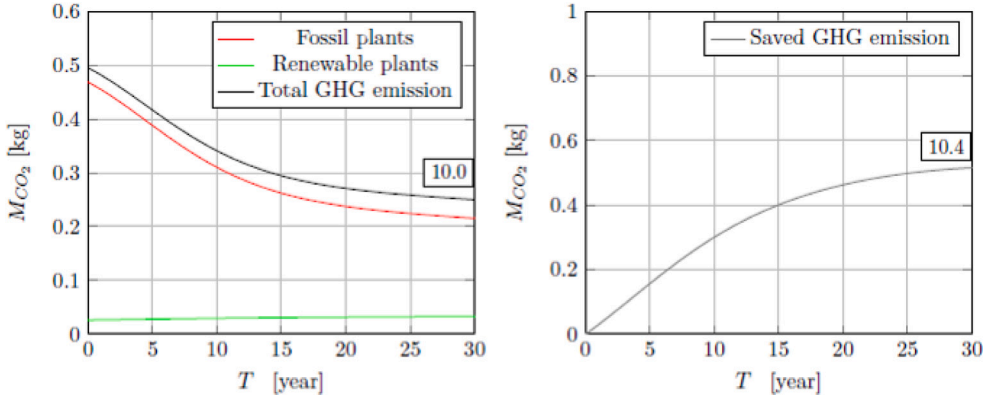

Fig. 47. GHG emission, scenario #16: degrowth rate: from $i = 4\%$ to $i = 2\%$. Boxed data indicate total GHG emissions [kg] of the whole period.

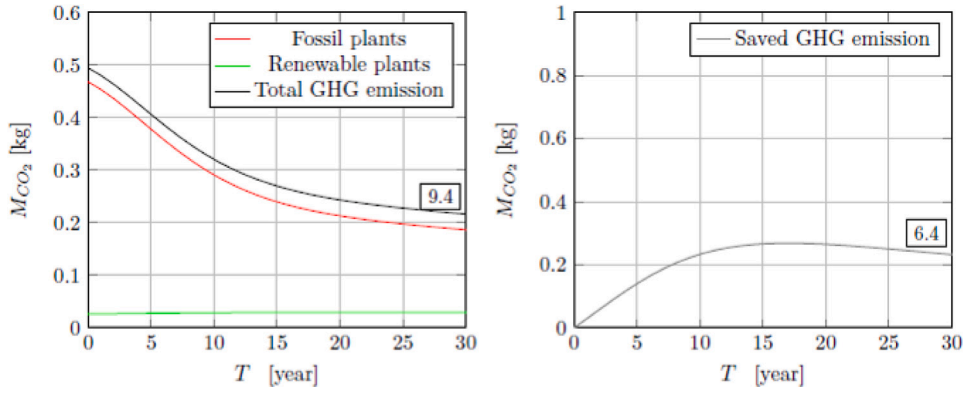

Fig. 48. GHG emission, scenario #17: complete degrowth rate from $i = 4\%$ to $i = 0.5\%$. Boxed data indicate total GHG emissions [kg] of the whole period.

advances that lead to an increase in the LF will reduce the power requirement from fossil fuels, though not so markedly. The figure also depicts the ideal case of $LF_{f,T30}$= 90%, to stress the concept that, even for this case the power reduction cannot fall below 50% of the power capacity of the baseline case.

Fig. 52 shows the same situation in relation to the load factor of renewable plants. Compared to the baseline case $LF_{r,baseline} = 20 \rightarrow 25\%$, the worst scenario is due to the constant load factor, which can depend on negligible technology advances or scarce loads interconnection, but also by the decision to develop low load factor technologies such as solar conversion plants (PV and thermal solar). Improvements in LF help to reduce the renewable plant capacity, and thus the land occupation. The ideal achievement of a load factor of 50%, which is feasible for countries that base their energy plans on a massive implementation of head hydropower and offshore wind energy, would reduce the required capacity from 72% down to 50% at the end of the period, compared to the baseline case.

Fig. 53 refers to scenarios of countries that start the transition process from different levels of fuel emission factors and considering a future reduction trend ($GHG_{f,2050} = 0.8 \cdot GHG_{f,2020}$), by considering future technology advancements, and the transition from low carbon to hydrogen fuels. Countries moving from a fuel mix that initially generates a 150% higher fuel emission factor (≈698 kg/kWh) compared to the baseline case, will end with +145% higher emissions (global emitted GHG of 15.5 kg, compared to about 10.4 kg given by the baseline scenario). The figure shows that the emissions vary linearly with the initial level of the fuel emission factor, all other factors being constant. The effect of the technology choice to contain future GHGs

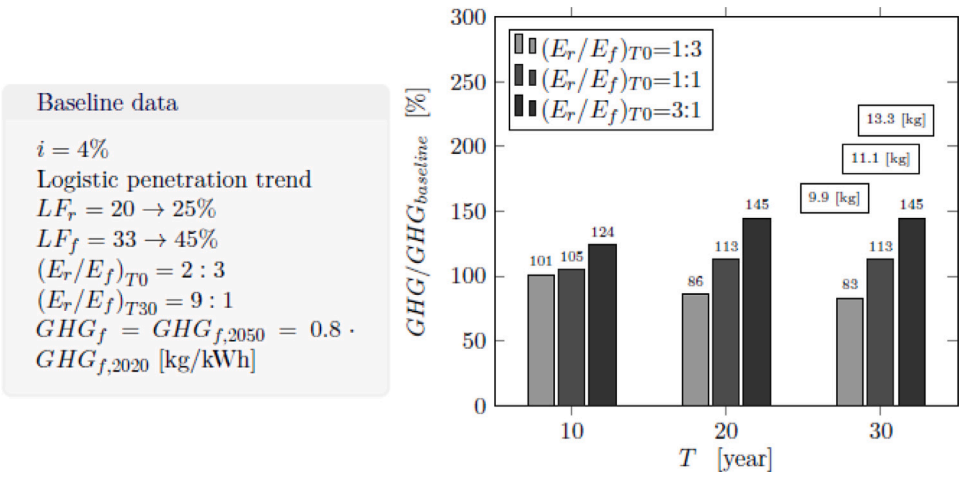

Fig. 49. Model sensitivity analysis: effect of renewable to fossil initial share $(E_r/E_f)_{f,T0}$ on $GHG/GHG_{baseline}$, Baseline data on the left box. Total GHG emitted in the whole period in the boxes above bars.

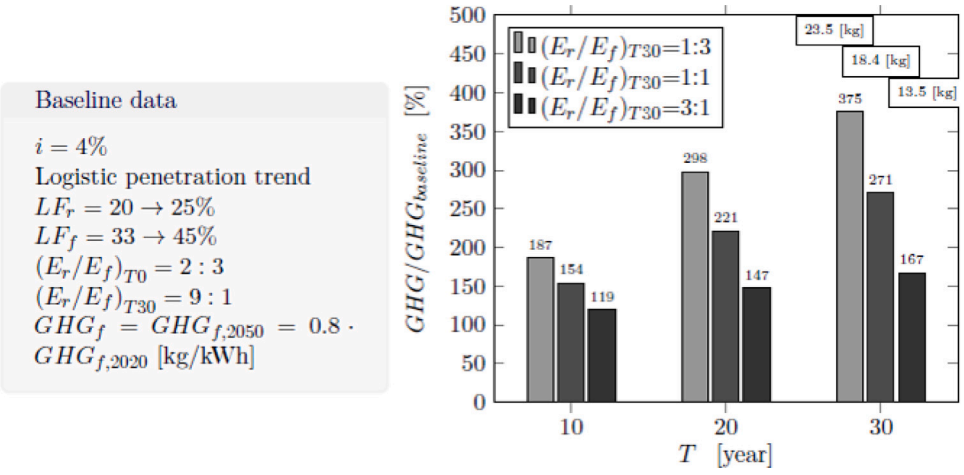

Fig. 50. Model sensitivity analysis: effect of renewable to fossil final share $(E_r/E_f)_{f,T30}$ on $GHG/GHG_{baseline}$, Baseline data on the left box. Total GHG emitted in the whole period in the boxes above bars.

from fossil fuels is shown in Fig. 54. Here two different fuel mixes are considered. The light fuels-high efficient situation ($GHG_{f,2050} = 0.6 \cdot GHG_{f,baseline}$), driven by the massive use of natural gas and combined power plants, leads to a reduction in emissions compared to today's levels, although this reduction is about 23% at the end of the period. The second situation investigated implies a massive return to the use of coal combustion ($GHG_{f,2050} = 1.3 \cdot GHG_{f,baseline}$). This determines an escalating trend in GHGs, with a final inventory that exceeds by about 40% the emissions of the light case.

7. Conclusion and policy implications

- Once the more likely scenario of future electricity demand has been chosen, the model allows determining the electric generation plant capacity and the related GHG emission, by the selection of input data as the emission parameters, the baseline data (renewable to fossil energy/power share), the baseline and future technical context, and the target energy transition path.
- the output of the power capacity required to satisfy a given energy scenario has an important impact on the programs of national energy plans, due to the time needed to locate, build and commission new power plant stations.
- each transition scenario indicates that very early (typically within the first transition quinquennial) the electricity produced from renewable sources exceeds that deriving from fossil fuels. Therefore a balancing problem of intermittent loads in the distribution network arises. These issues can be solved with electricity storage systems, smart loads management, and electric grid interconnection. However, it is unlikely to be solved for many countries within the time frame foreseen in the transition scenarios due to the infrastructural effort needed;
- 'total' penetration of 90% of renewable sources in the electricity generation system, and under the auspices of the best technological advances, does not lead to a corresponding reduction of 90% in GHGs level;
- 'total' electric energy decrease, with a growing rate that falls from 4% to 0.5%, leads to emissions reduction by only 55% compared to today's data;
- technological advances alone cannot solve the problem of future emissions unless accompanied by an electric energy consumption reduction strategy, as proved from simulations including strong improvements in energy conversion technology (increasing LF scenarios);
- Considering realistic growth scenarios and regardless of the penetration rate expected by renewable sources, each transition scenario still entails relying on significant levels of fossil fuel power. The recent history of the energy consumption of industrialized countries confirms that the progressive penetration of renewables

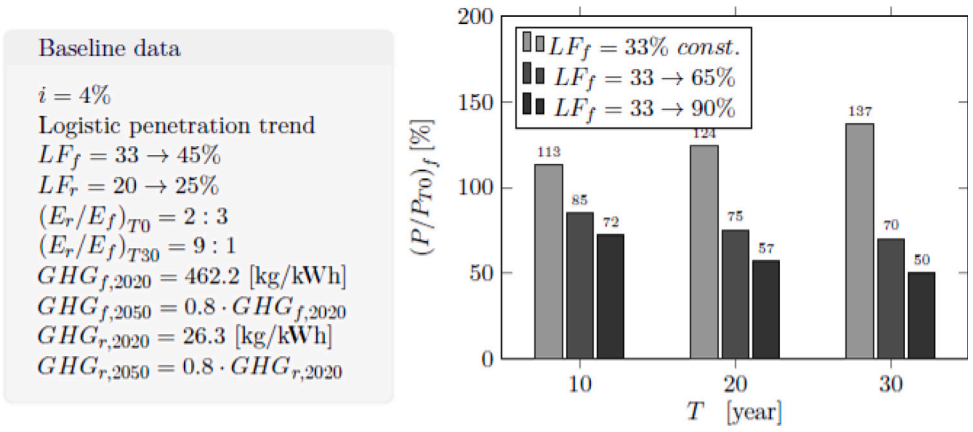

Fig. 51. Model sensitivity analysis: effect of LF_f evolution on fossil power $(P/P_{T0})_f$, Baseline data on the left box.

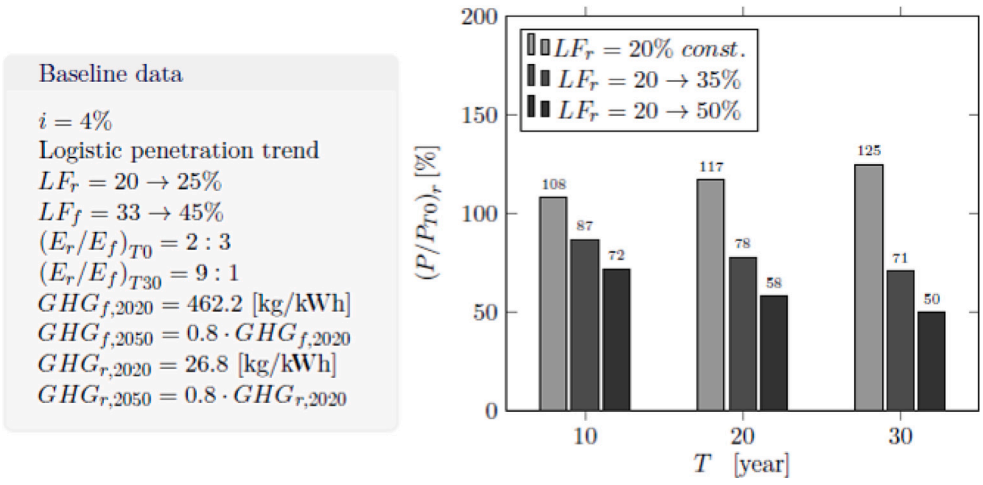

Fig. 52. Model sensitivity analysis: effect of $GHG_{f,T0}$ on $GHG_{f,baseline}$ data on the left box. Total GHG emitted in the whole period in the boxes above bars.

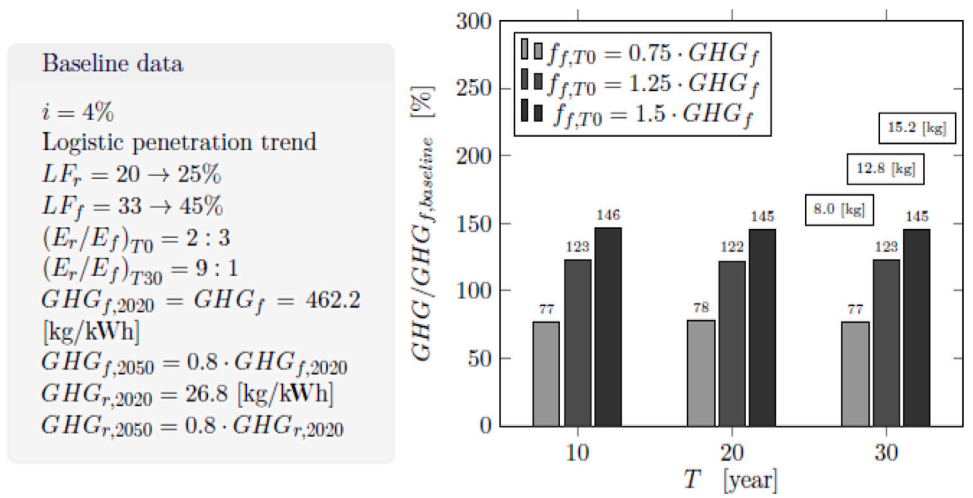

Fig. 53. Model sensitivity analysis: effect of $GHG_{f,T0}$ on $GHG_{f,baseline}$ data on the left box. Total GHG emitted in the whole period in the boxes above bars.

has never led to a marked reduction of electrical energy produced by fossil sources. Standing current and foreseen electric energy growth demands, renewables cannot definitively perform the desired 'replacement' function but instead are likely to be

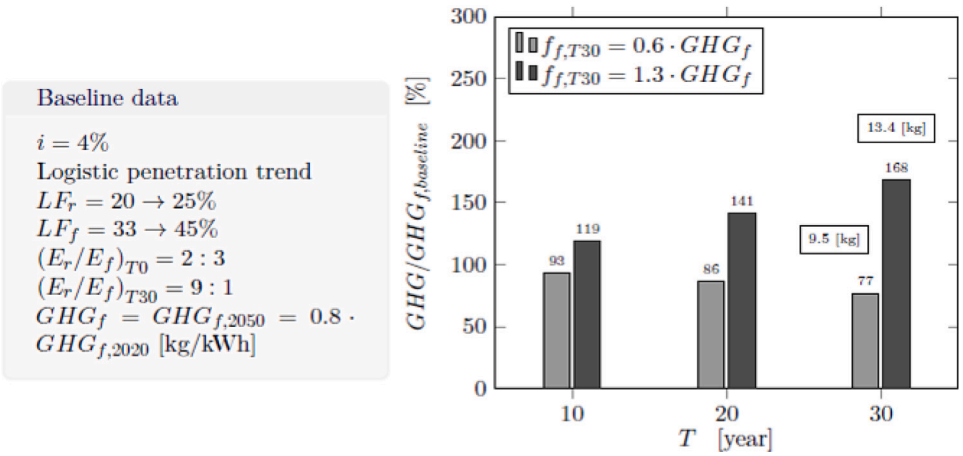

Fig. 54. Model sensitivity analysis: effect of $GHG_{f,T30}$ on $GHG_{f,baseline}$ data on the left box. Total GHG emitted in the whole period in the boxes above bars.

an 'integration' factor of an ever-increasing demand for capacity. These facts indicate that the adjective 'alternative' should no longer be used for renewable sources.

CRediT authorship contribution statement

L. Battisti: Conceptualization, Methodology, Software, Validation, Investigation, Resources.

Declaration of competing interest

The authors declare the following financial interests/personal relationships which may be considered as potential competing interests: Lorenzo Battisti reports administrative support was provided by University of Trento. Lorenzo Battisti reports a relationship with University of Trento that includes: employment. none.

Data availability

No data was used for the research described in the article.

References

Agency, E.E.E., 2015. Renewable energy in Europe – approximated recent growth and knock-on effects. (Accessed 25 January 2022).

American, Scientific, 2018. Global co_2 emissions rise after Paris climate agreement signed. URL: https://www.scientificamerican.com/article/global-co2-emissions-rise-after-paris-climate-agreement-signed/. (Accessed 20 January 2022).

Ang, B., 2004. Decomposition analysis for policymaking in energy: which is the preferred method? Energy Policy 32, 1131–1139.

Arera, 2019. Stato Di Utilizzo e di Integrazione Degli Impianti Di Produzione Alimentati Dalle Fonti Rinnovabili e di Generazione Distribuita. Autorità Di Regolazione Per Energia, Reti E Ambiente Relazione 321/2020/I/Efr. Dati 2019.

Becker, M., Meinecke, W., 1992. Solarthermische Anlagen-Technologien im Vergleich. Springer-Verlag, Berlin, Heidelberg, New York.

Bonou, A., Laurent, A., Olsen, S., 2016. Life cycle assessment of onshore and offshore wind energy-from theory to application. Appl. Energy 180, 327–337.

Bouman, E.A., 2020. A Life Cycle Perspective on the Benefits of Renewable Electricity Generation. Eionet Report - ETC/CME 4/2020.

BP, 2020. Statistical Review of World Energy 2020. Vol. 10, 69th ed. pp. 345–356, URL: https://www.bp.com/content/dam/bp/business-sites/en/global/corporate/pdfs/energy-economics/statistical-review/bp-stats-review-2020-full-report.pdf.

Burke, D., O'Malley, M., 2011. Factors influencing wind energy curtailment. IEEE Trans. Sustain. Energy 2, 185–193. http://dx.doi.org/10.1109/TSTE.2011.2104981.

C2ES, 2021. Center for climate and energy solutions. Global emissions. URL: https://www.c2es.org/content/internationalemissions/. (Assessed 25 October 2021).

Clancy, J., Gaffney, F., Deane, J., Curtis, J., Gallachóir, B., 2015. Fossil fuel and CO2 emissions savings on a high renewable electricity system – a single year case study for Ireland. Energy Policy 83, 151–164.

Cochran, J., Miller, M., et al., 2014. Flexibility in 21st Century Power Systems. NREL/TP-6A20-61721, National Renewable Energy Laboratory (NREL).

DeutscheWelle, 2020. Tackling climate change from Kyoto to Paris and beyond. URL: https://www.dw.com/en/kyoto-protocol-climate-treaty/a-52375473. (Accessed 3 January 2022).

Dudhani, S., Sinha, A., et al., 2006. Renewable energy sources for peak load demand management in India. Int. J. Electr. Power 28 (6), 396–400.

EEA, 2021. Total greenhouse gas emission trends and projections in Europe. URL: https://www.eea.europa.eu/ims/total-greenhouse-gas-emission-trends.

EIA, 2022. Annual electric generator report. Form EIA-860 Detailed Data with Previous Form Data (EIA-860A/860B). URL: https://www.eia.gov/electricity/data/eia860/.

El-Fadel, M., Chedid, R., et al., 2003. Mitigating energy-related GHG emissions through renewable energy. Renew. Energy 28 (8), 1257–1276.

nd Energiewende, A., Ember, 2021. The European power sector in 2020: Up-to-date analysis of the electricity transition, version 1.0.. AEE. 202/02-a-2021/EN. URL: https://www.iea.org/reports/net-zero-by-2050.

EU, 2021. Delivering the European green deal. European and Commission. URL: https://ec.europa.eu/info/strategy/priorities-2019-2024/european-green-deal/delivering-european-green-deal_en.

Gagnona, L., Bélanger, C., Uchiyama, Y., 2002. Life-cycle assessment of electricity generation options: The status of research in year 2001. Energy Policy 30, 1267–1278.

Goh, T., Ang, B., 2018. Quantifying CO2 emission reductions from renewables and nuclear energy - Some paradoxes. Energy Policy 113, 651–662.

del Granado, P.C., van Nieuwkoop, R., Kardakos, E., Schaffner, C., 2018. Modelling the energy transition: A nexus of energy system and economic models. Energy Strategy Rev. 20, 229–235.

Halbe, J., Reusser, D., Holtz, G., M., H., Stosius, A., Avenhaus, W., Kwakkel, J., 2015. Lessons for model use in transition research: A survey and comparison with other research areas. Environ. Innov. Societal Transitions 15, 194–210.

Hammons, T.J., 2004. Geothermal power generation worldwide: Global perspective, technology, field experience, and research and development. Electr. Power Compon. Syst. 35 (2), 529–553.

Helton, J., Johnson, J.D., Sallaberry, C., Storlie, C., 2006. Survey of Sampling-Based Methods for Uncertainty and Sensitivity Analysis. Sandia Report SAND2006-2901.

Holttinen, H., Kiviluoma, J., Cantor, C., Mccann, J., Clancy, M., Eigan, M., 2014. Estimating the reduction of generating system CO2 emissions resulting from significant wind energy penetration. In: 13thWind Integration Workshop. URL: https://www.researchgate.net/publication/265685383.

Hondo, H., 2005. Life cycle GHG emission analysis of power generation systems: Japanise case. Energy 30, 2042–2056.

IEA, 2019. Global Share of Electricity Generation. International Energy Agency, URL: https://www.iea.org/data-and-statistics/charts/global-share-of-electricity-generation-2019.

IEA, 2020. Energy efficiency 2020. Form EIA-860 Detailed Data with Previous Form Data (EIA-860A/860B). URL: https://www.iea.org/reports/energy-efficiency-2020.

IEA, 2021a. Global Energy Review 2021. International Energy Agency, URL: https://www.iea.org/reports/global-energy-review-202.

IEA, 2021b. Net Zero by 2050. International Energy Agency, URL: https://www.iea.org/reports/net-zero-by-2050.

IEA, 2021c. Global energy review: CO2 emissions in 2020. URL: https://www.iea.org/articles/global-energy-review-co2-emissions-in-2020. (Accessed 25 January 2022).

Impram, S., Nese, S., Oral, B., 2020. Challenges of renewable energy penetration on power system flexibility: A survey. Energy Strategy Rev. 31 100539, 519–522.

IPCC, 2006. IPCC Guidelines for National Greenhouse Gas Inventories, Prepared by the National Greenhouse Gas Inventories Programme. IGES, Japan, The Intergovernmental Panel on Climate Change.

IPCC, 2014. Climate Change 2014: Mitigation of Climate Change. Contribution of Working Group III to the Fifth Assessment Report of the Intergovernmental Panel on Climate Change. Cambridge University Press, Cambridge, United Kingdom and New York, NY, USA, The Intergovernmental Panel on Climate Change.

IPCC, 2018. Special report on global warming of 1.5° C. The Intergovernmental Panel on Climate Change. URL: https://www.ipcc.ch/sr15/.

IPCC, 2021. Refinement to The 2006 IPCC Guidelines For National Greenhouse Gas Inventories - The Physical Science Basis. Contribution of Working Group I to the Sixth Assessment Report of the Intergovernmental Panel on Climate Change. Cambridge University Press, URL: https://www.ipcc.ch/report/2019-refinement-to-the-2006-ipcc-guidelines-for-national-greenhouse-gas-inventories/.

ISO, 2006. ISO 14040:2006 Environmental management, Life cycle assessment — Principles and framework. Int. J. Life Cycle Assess. Edition 2 Number of pages: 20, Technical Committee: ISO/TC 207/SC 5 Life cycle assessment, and following amendments ISO 14040:2006/AMD 1:2020. ICS : 13.020.10 Environmental management 13.020.60 Product life-cycles.

ISPRA, 2021a. Indicatori Di Efficienza E Decarbonizzazione Del Sistema Energetico Nazionale E Del Sistema Elettrico. Rapporti 343/2021, Istituto Superiore per la Ricerca e la Protezione ambientale.

ISPRA, 2021b. Italian Greenhouse Gas Inventory 1990–2019. National Inventory Report 2021. Rapporti 341/2021, Cambridge University Press, Istituto Superiore per la Ricerca e la Protezione ambientale.

Kabir, M., Rooke, B., Dassanayake, G., Fleck, B., 2012. Comparative life cycle energy, emission, and economic analysis of 100 kW nameplate wind power generation. Renew. Energy 37, 133–141.

Kim, S., Kim, S., 2016. Decomposition analysis of the greenhouse gas emissions in Korea's electricity generation sector. Carbon Manag. 7, 249–260.

Latouche, S., 2010. Degrowth. J. Clean. Prod. 18 (6), 519–522. http://dx.doi.org/10.1016/j.jclepro.2010.02.003.

Lenzen, M., Munksgaard, J., 2002. Energy and CO2 life-cycle analyses of wind turbines—review and applications. Renew. Energy 26, 339–362. http://dx.doi.org/10.1016/S0960-1481(01)00145-8.

Li, F., Trutnevyte, E., Strachan, N., 2015. A review of socio-technical energy transition (STET) models. Technol. Forecasting Soc. Chang. 100, 290–305.

de Lima, G., Toledo, A., Bourikas, L., 2021. The role of national energy policies and life cycle emissions of PV systems in reducing global net emissions of greenhouse gases. Energies 14 961, http://dx.doi.org/10.3390/en14040961.

Marchetti, C., 1977. Primary energy substitution models: On the interaction between energy and society. Technol. Forecast. Soc. Change 10, 345–356.

Meadows, D., Randers, J., III, W.B., 1972. The Limits to Growth. NewAme Rican Library, New York.

Müllera, B., Gardumi, F., Hülk, L., 2017. Comprehensive representation of models for energy system analyses: Insights from the Energy Modelling Platform for Europe (EMP-E). Energy Strategy Rev. 21, 82–87.

Nakicenovic, N., et al., 2000. Special report on emissions scenarios: a special report of working group III of the intergovernmental panel on climate change. URL: https://www.ipcc.ch/site/assets/uploads/2018/03/sres-en.pdf.

Nishimura, A., Hayashi, Y., Tanaka, K., Hirota, M., Kato, S., Ito, M., Araki, K., Hu, E., 2010. Life cycle assessment and evaluation of energy payback time on high-concentration photovoltaic power generation system. Appl. Energy 87, 2797–2807.

Pearl, R., Reed, L., 1920. On the rate of growth of the population of the United States since 1790 and its mathematical representation. Proc. Nat. Acad. Sci. 6, 275–288.

Peng, J., Lu, L., Yang, H., 2013. Review on life cycle assessment of energy payback and greenhouse gas emission of solar photovoltaic systems. Renew. Sustain. Energy Rev. 19, 255–274.

Pollin, R., 2018. De-growth vs a new green deal. New Left Rev. 112, July-Aug. 2018.

Reap, J., Roman, F., Duncan, S., Bras, B., 2008. A survey of unresolved problems in life cycle assessment Part 2: impact assessment and interpretation. Int. J. Life Cycle Assess 13, 374–388. http://dx.doi.org/10.1007/s11367-008-0009-9, 275–288.

Smil, V., 2015. Power Density: A Key to Understanding Energy Sources and Uses. The MIT Press, Cambridge, MA.

TERNA, 2020. Dati statistici 2020. URL: https://www.terna.it/it/sistema-elettrico/statistiche/pubblicazioni-statistiche.

Torvanger, A., 1991. Manufacturing sector carbon dioxide emissions in nine OECD countries: 1973–87. Energy Econ. 13, 168–186.

Tudor, C., Sova, R., 2021. Benchmarking GHG emissions forecasting models for global climate policy. Electronics 10,3149, http://dx.doi.org/10.3390/electronics10243149.

UN, 2021. Emissions Gap Report 2021. Emissions Gap Report (EGR) 2021, URL: https://www.unep.org/resources/emissionsgap-report-2021.

UNCCC, 2019. Cut global emissions by 7.6 percent every year for next decade to meet 1.5° C Paris target. URL: https://unfccc.int/news/cut-global-emissions-by-76-percent-every-year-for-next-decade-tomeet-15degc-paris-target-un-report.

UNCCC, 2021. Nationally determined contributions (NDCs). https://unfccc.int/process-and-meetings/the-paris-agreement/nationally-determined-contributions-ndcs/nationally-determined-contributionsndcs. (Accessed 5 January 2022).

UNFCCC, 2021a. Nationally Determined Contributions Under the Paris Agreement. UNFCCC - and United and Nations and Framework and Convention and on and Climate and Change, URL: https://unfccc.int/sites/default/files/resource/cma2021_08_adv_1.pdf. (Accessed 3 January 2022).

UNFCCC, 2021b. The Paris Agreement. UNFCCC - and United and Nations and Framework and Convention and on and Climate and Change, https://unfccc.int/process-and-meetings/the-paris-agreement/the-paris-agreement. (Accessed 3 January 2022).

Varun, I.K., Bhat, R., 2009. LCA of renewable energy for electricity generation systems - A review. Renew. Sustain. Energy Rev. 13, 1067–1073.

Wang, Y., Sun, T., 2012. Life cycle assessment of CO2 emissions from wind power plants: Methodology and case studies. Renew. Energy 43, 30–36.

Wen, L., Yuan, X., 2020. Forecasting co_2 emissions in Chinas commercial department, through BP neural network based on random forest and PSO. Sci. Total Environ. 718, 137194.

White, S., Kulcinski, G., 2000. Birth to death analysis of the energy payback ratio and CO2 gas emission rates from coal, fission, wind, and DT-fusion electrical power plants. Fusion Eng. Des. 48, 473–481.

Xu, X., Ang, B., 2013. Index decomposition analysis applied to CO2 emission studies. Ecol. Econ. 93, 313–329.

Xu, X., Ang, B., 2014. Multilevel index decomposition analysis: approaches and application. Energy Econ. 44, 375–382.

Yang, J., Hao, Y., Feng, C., 2011. A race between economic growth and carbon emissions: What play important roles towards global low-carbon development? Energy Econ. 100, 105327.

Zhang, M., Liu, X., Wang, W., Zhou, M., 2013. Decomposition analysis of CO2 emissions from electricity generation in China. Energy Policy 52, 159–165.